Galaxy Populations and Evolution in Clusters IV: Deep HI Observations of Dwarf Ellipticals in the Virgo Cluster

Christopher J. Conselice[1], Karen O'Neil[2], John S. Gallagher[3], Rosemary F.G. Wyse[4]

Draft February 27, 2003

ABSTRACT

In this paper we present deep Arecibo HI and WIYN optical observations of Virgo cluster dwarf ellipticals. Based on this data we argue that some low-mass galaxies in the Virgo cluster recently underwent evolution. Our new observations consist of HI 21-cm line observations for 22 classified dE galaxies with optical radial velocities consistent with membership in the Virgo cluster. Cluster members VCC 390 and VCC 1713 are detected with HI masses $M_{HI} = 6 \times 10^7\ M_\odot$ and $8 \times 10^7\ M_\odot$, respectively, while M_{HI} in the remaining 20 dE galaxies have upper limits as low as $\sim 5 \times 10^5\ M_\odot$. We combine our results with those for 27 other Virgo cluster dEs with HI observations in the literature, 7 of which have HI detection claims. New optical images from the WIYN telescope of 5 of these HI-detected dEs, along with archival data, suggest that seven of the claimed detections are true HI detections, yielding a ≈15% detection rate. These HI-detected classified dEs are preferentially located near the periphery of the Virgo cluster. Three Virgo dEs have observed HI velocity widths > 200 km s^{-1}, possibly indicating the presence of a large dark matter content, or transient extended HI. We discuss the possible origins of these objects and argue that they originate from field galaxies accreted onto high angular momentum orbits by Virgo in the last few Gyr. As a result of this we argue that these galaxies are slowly transformed within the cluster by gradual gas stripping processes, and associated truncation of star formation, and passive fading of stellar populations. Low-mass early-type cluster galaxies are therefore

[1]California Institute of Technology, Mail Code 105-24, Pasadena CA. 91125

[1]NSF Astronomy & Astrophysics Postdoctoral Fellow

[2]Arecibo Observatory, HC3 Box 53995, Arecibo, PR. 00612

[3]Department of Astronomy, The University of Wisconsin-Madison, Madison WI. 53706

[4]Department of Physics and Astronomy, Johns Hopkins University, Baltimore MD. 21218

currently being produced as the product of cluster environmental effects. We utilize our results in a simple model to estimate the recent (past 1-3 Gyr) mass accretion rate into the Virgo cluster, deriving a value of $\dot{\rm M} \sim 50$ $M_\odot$ year^{-1}.

1. Introduction

Low-mass cluster galaxies (LMCGs), including objects classified as dwarf ellipticals (dEs, Ferguson & Binggeli 1994), dwarf spheroidals (Gallagher & Wyse 1994), and irregulars (Gallagher & Hunter 1984) hold many clues for understanding galaxy formation and evolution. These are the most common galaxies in the nearby universe (e.g., Ferguson & Binggeli 1994), and may be the first galaxies formed (e.g., Blumenthal et al. 1984; White & Frenk 1991). The relative number densities of dwarfs also increases with local galaxy density (e.g., Trentham, Tully, & Verheijen 2001) with a particularly high abundance found in galaxy clusters, including Virgo (Binggeli, Tammann & Sandage 1985; hereafter the Virgo Cluster Catalog or VCC). As such LMCGs offer an outstanding opportunity to understand the origin of the lowest mass systems in the universe.

The origins of LMCGs are still a mystery. Star-forming LMCGs, usually classified as dwarf irregulars, are probably recent additions to galaxy clusters (e.g., Gallagher & Hunter 1989; Conselice, Gallagher & Wyse 2001a, hereafter Paper I) as indicated by their high gas content, recent star formation, and kinematic characteristics (Paper I). Quiescent LMCGs, including dEs[6], are low mass ($< 10^9$ $M_\odot$), low luminosity ($M_B > -17$), low surface-brightness ($\mu_B > 24$ mag arcsec^{-2}) objects with little to no HI gas (Ferguson & Binggeli 1994). Despite their faintness, these early-type LMCGs are more common than their star-forming dIrr counterparts, and likely contain a mix of stellar population ages and metallicities, and thus possibly reflect a variety of origins (e.g., Ferguson & Binggeli 1994; Conselice, Gallagher & Wyse 2002a,b; Papers II & III). This paper focuses on understanding the dE-like LMCGs seen in the Virgo Cluster by searching for HI gas that might be left over from their progenitors (see Paper III for a detailed discussion of possible formation scenarios).

---

[6]The term dwarf elliptical (dE) is sometimes used in this paper to describe low-mass objects without recent star formation, and with apparently symmetric structures. Dwarf spheroidals are a sub-set of dwarf ellipticals with faint magnitudes and low surface brightnesses (Gallagher & Wyse 1994). In our view these two terms are interchangeable, and we include both in the general dE designation. To not bias the interpretation of what Virgo objects with HI detections are, we use the term low-mass cluster galaxy (LMCG) to describe them, even though these objects have been classified by others (e.g,. Binggeli et al. 1985) as dwarf ellipticals.

Due to their low masses and apparently old stellar populations dwarf elliptical/spheroidal galaxies in the local universe are outstanding candidates for being among the first galaxies to form. Another scenario is that dEs formed after the cluster's initial collapse (see Paper I & III), possibly originating from accreted field galaxies. It is however not yet known with certainty (cf. Vigroux et al. 1986; Gallagher & Hunter 1989) if there are any galaxies in nearby clusters that are currently undergoing morphological transitions from spiral $\rightarrow$ dE, dIrr $\rightarrow$ dE, or spiral + spiral $\rightarrow$ elliptical, although inducing these transformations by merging within clusters today is unlikely due to the high relative velocities of cluster members (cf. Conselice et al. 2001b). Dwarf elliptical formation is however potentially still ongoing.

One way to search for objects undergoing formation/evolution into an early-type LMCG is to look for galaxies that morphologically appear as dEs, but have properties suggesting recent evolution from star-forming, and possibly more massive systems, such as irregulars or low-mass spirals. These signs include younger and/or metal enriched stellar populations (Paper III) and significant atomic gas. We call these galaxies, containing properties of several galaxy types, LMCG transition objects. In this paper, we present results from a survey for HI 21-cm line emission from Virgo early-type LMCGs. We discover two candidate HI-rich dEs from a sample of 22 observed with the Arecibo 305-m telescope, which we add to the 7 candidate Virgo Cluster dEs with HI detections published in the literature. These HI-detected LMCGs have inferred gas fractions that are high, placing them in the realm of dwarf irregular or Local Group transition-type dwarfs, but have morphologies consistent with dwarf elliptical objects (Binggeli et al. 1985). Based on an analysis of these properties we conclude that seven of these LMCGs are likely transition objects, morphologically evolving into early-type dwarfs from star-forming systems.

This paper is organized as follows: §2 discusses our new observations, §3 presents our basic results after combining our new data with previously published findings, §4 gives interpretations of our results, §5 gives an estimation of the current accretion rate into Virgo and §6 is a summary. A Virgo cluster distance of 18 Mpc is assumed throughout this paper, giving a scale of $\sim$ 5 kpc arcmin^{-1}.

2. Observations and Sample

The new HI observations we present were taken with the Arecibo 305 meter radio telescope in April and May 2001. We observed 22 Virgo LMCGs classified as dEs by Binggeli et al. (1985) (see Table 1). This sample of observed objects was chosen from the list of all classified dEs in Virgo with known radial velocities, compiled and listed in Paper

I. To be observed, an object had to be relatively bright, with an apparent magnitude of B < 17 ($M_B < -14.0$). From these systems, a random set of 22 objects classified as dEs, or 23% of the total number with known radial velocities covering the range of Virgo dEs (Paper I), were chosen for 21-cm observations (Table 1). The sample of observed objects is also spread over the entire angular extent of the Virgo cluster, as defined in the VCC.

Our 21-cm observations were taken using the Arecibo L-Narrow Gregorian receiver. The four Arecibo correlator channels were all centered on the HI (21-cm) line, based on the optical determined radial velocities (Paper I). Two different bandwidths were simultaneously observed, with widths 6.25 MHz and 12.5 MHz, at two different circular polarizations. Observations were made with 9-level sampling, giving each board 2048 channels and providing us with an unsmoothed resolution of 0.65 and 1.3 km s^{-1} for the two different bandwidths, respectively. Each target was observed using standard position-switching techniques, with each five minute on-source observation followed by a five minute 'blank sky' observation, which tracked the same azimuth-zenith angle position of the reflector. Each on+off pair was followed by an observation of a standard noise diode for temperature calibration. All data were obtained at night to eliminate solar interference.

During each night we also observed strong continuum sources to check the observatory supplied gain curve. All calibration sources were chosen to be non-variable, and to have sizes < 10% of the beam width. The flux scales for each source are based on the calibrations from Baars et al. (1977) and Kuehr et al. (1981). We also observed galaxies of small angular size with published HI line profiles from the list in Lewis, Helou & Salpeter (1985). These measurements were done to confirm the accuracy of the internal line flux and frequency calibration. Table 1 lists the integration times and 3σ detection limits in the HI spectrum of each object we observed. On source integration times ranged from 0.6 ks to 5.7 ks.

We reduced all of our HI observations using ANALYZ, the Arecibo data analysis program (O'Neil 2003 in prep). To obtain fluxes, velocity widths and other information for our two new detections, VCC 390 and VCC 1713 (Table 2), first order baselines were subtracted from the observed spectra. The baselines were fitted interactively and then removed from the HI line profile. Both single and double Gaussians were then fit to the HI lines. These profiles were fit within the area that occupies the HI emission. That is, we start and end the fit where the line distinguishes itself from the noise. Since this is ultimately somewhat of a subjective process, we repeated it several times to obtain an estimated random error. This fitting process gives line widths at 20% and 50% of the peak brightness, as well as the total flux in each HI line.

3. Results

3.1. HI Properties

Of the 22 galaxies we observed at Arecibo, only 2 have significant HI detections (Figure 1). This is not an exceptionally low rate, since many previous observations also found few, to no, detections of HI in Virgo cluster galaxies classified as dEs (e.g., Huchtmeier & Richter 1986; Bothun et al. 1985). We supplemented our sample by performing a literature search to find other classified Virgo dEs with HI detections; a further seven objects with 21-cm detection claims were retrieved. We discuss these seven objects in §3.5. Table 2 lists all of the Virgo cluster dwarfs classified as dEs observed to date at 21-cm.

Since the new observations presented here are the most sensitive ever taken, we might expect a higher fraction of detections if HI gas was commonly found in early-type LMCGs. There are 97 Virgo galaxies classified as dwarf elliptical galaxies with measured stellar radial velocities (Paper I) and 49 (51%) of these have been observed in the 21-cm line. Of these, 9 (19% of the total) have claimed HI detections. Through the following analysis we conclude that one of these detections is not significant enough to be considered real (VCC 405) and we argue that the other is a dwarf irregular galaxy (VCC 2082). All of the published HI detections, including our two new objects, are listed in Table 3.

3.1.1. HI Masses

We used the flux of the 21-cm line to determine HI gas masses for each detected LMCG through the formula,

$$\mathrm{M_{HI}}(\mathrm{M_\odot}) = 2.36 \times 10^5 D(\mathrm{Mpc})^2 \int \mathrm{S}(\nu)\, d\nu, \tag{1}$$

where D is the distance to the galaxy in Mpc, in our case assumed fixed at 18 Mpc, and $\int$ S(ν) $d\nu$ is the integral of the flux in units of Jy km s^{-1}. For the undetected galaxies we observed at Arecibo, we set limits on HI masses (Table 1) by assuming a 3σ detection limit over 60 km s^{-1}. This provides an average HI upper limit mass of $\sim 8\times10^6$ M$_\odot$. Our deepest observation was for the galaxy VCC 543, where we reach a 3σ limit in the 12.5 MHz band of 0.002 mJy channel^{-1}, corresponding to a 3σ upper mass limit of 4.6×10^5 M$_\odot$.

With these limits we are reaching the detectability threshold of some Local Group dwarf ellipticals and spheroidals. For example, the dwarf ellipticals NGC 205 and NGC 185 have HI masses 3.4×10^5 M$_\odot$ and 1.3×10^5 M$_\odot$ respectively (Young & Lo 1997; Johnson

& Gottesman 1993). Dwarf irregular galaxies such as IC 10 and IC 1613, with HI masses of 1.2×10^8 $M_\odot$ and 6.5×10^7 $M_\odot$ (Huchmeier 1979; Volders & Högborn 1961), would easily be detected in our survey. Even the faintest Local Group dwarf irregular, the Sagittarius DIG, has an HI gas content of 1.1×10^7 $M_\odot$ and would be easily detectable at the distance of Virgo in our survey.

However, a few Local Group dwarf spheroidals, such as NGC 147 still remain undetected in HI, down to a limit of $\sim 3 \times 10^3$ $M_\odot$ (Young 1999), and many of the objects we observe with no detections could have equally low HI gas masses. Fainter dwarf spheroidals, such as Fornax and Leo II, also have extremely low HI mass upper limits of $< 10^4$ $M_\odot$ (Young 1999).

3.2. Optical Images

Figure 2 shows the second generation Digitized Sky Survey (DSS) images for all nine early-type LMCGs with reported HI detections. This field size was chosen to match the Arecibo beam, but detections using other telescopes had different beam sizes. In several cases, e.g., VCC 405, nothing obvious is seen, demonstrating that some objects are very faint. In most cases, however, it is clear that these LMCGs are smooth objects with very little structural evidence for active star formation, consistent with their classification as dwarf ellipticals by Binggeli et al. (1985).

We also acquired WIYN 3.5 meter broad-band Harris R images for five of the nine Virgo HI detected LMCGs (VCC 31, VCC 168, VCC 390, VCC 797, VCC 1713). These shallow images were taken under non-photometric conditions using the Mini-Mosaic CCD, which has a field of view $9.6' \times 9.6'$. Mini-Mosaic consists of two SITe 4096×2048 pixel CCDs separated by a gap of $5''$ and a pixel scale of $0.14''$ pixel^{-1} (see Paper II for a further description of Mini-Mosaic). The typical exposure times for these five images were 500 seconds, suitable for obtaining morphological and structural information.

The five HI detected LMCGs imaged with WIYN are shown in Figure 3. With the possible exception of VCC 1713 these galaxies all appear to be quiescent early-type LMCGs, confirming the impression from Figure 2. Figure 3 also shows the surface brightness profiles for these five LMCGs with an arbitrary normalization. Table 4 lists the quantitative morphological properties for these galaxies, including the asymmetry, A, (Conselice 1997; Conselice et al. 2000a,b), concentration, C, (Bershady, Jangren & Conselice 2000), clumpiness index, S, (Conselice 2003), as well as the Sérsic profile index and scale radius, n and r_0, according to the formula, $\mathrm{I} = \mathrm{I_0} \exp(-(\mathrm{r}/\mathrm{r_0})^{1/n})$ (see Paper III for details).

The asymmetry parameter, A, is a measure of how asymmetric a galaxy is found by quantifying the residuals after rotating a galaxy's image 180° by its center and subtracting this new image from the original (Conselice et al. 2000a). Most early-type galaxies have $A \sim 0$. The concentration parameter, C, is a measure of how concentrated the light in a galaxy is towards its center. Most ellipticals have $C > 3.5$, while disks and dwarf galaxies have lower values from $2 < C < 3$ (Bershady et al. 2000). The clumpiness index, S, is found by quantifying the fraction of spatial high frequency light in a galaxy. Most early type galaxies have very little high spatial frequency structure, and thus have clumpiness values $S \sim 0$. Table 4 is consistent with the visual impression of these as early-type galaxies.

3.3. Dynamical Masses and $\mathrm{M_{dyn}/L_B}$ Ratios

Although we cannot make any firm dynamical mass claims, we can compute some estimates based on the likely physical conditions of each LMCG with an HI detection (Table 3). A major problem in computing dynamical masses for these galaxies is deciding what radius corresponds to the measured velocity width, and what component of the single gaussian line-widths are due to rotation, velocity anisotropy, and random turbulent motion. To estimate dynamical masses, we assume that the HI velocity width represents rotation on orbits that are nearly circular, plus some turbulence. Observations show that the HI sizes of galaxies can be much bigger than their optical sizes (e.g., Broeils 1992; van Zee, Skillman & Salzer 1998), although some Virgo galaxies have truncated HI profiles (e.g., Haynes & Giovanelli 1986). For a size, we use the optical radius estimates for these galaxies given in the VCC, and listed in Table 3. We also assume the circular velocity ($\mathrm{V_{rot}}$) to be half the HI line velocity width at 50% maximum, $\mathrm{W_{50}}$, uncorrected for inclination, from our HI spectroscopy. Normally we would use the $\mathrm{W_{20}}$ velocity widths, but these values are not available for many of the galaxies listed in Table 2. Using $\mathrm{W_{50}}$ instead of $\mathrm{W_{20}}$ reduces the dynamical mass, and mass to light ratios, by an average of ~70%, and increases the HI mass fraction by the same amount (Table 3). We compute lower limits to dynamical masses using the equation:

$$\mathrm{M_{dyn}} \geq \mathrm{V_{rot}^2} \times \mathrm{R/G} \sim 0.25 \times \mathrm{W_{50}^2} \times \mathrm{R/G} \tag{2}$$

where we have used the approximation $\mathrm{V_{rot}} = (\mathrm{W_{50}}/2)$ with the derived masses listed in Table 3. The radii we use are from Binggeli et al. (1985) and are also listed in Table 3. From these values we are able to compute dynamical mass to light ratios, $(\mathrm{M_{dyn}/M_B})$, and gas mass fractions, $\mathrm{f_{gas}} = \mathrm{M_{HI}/M_{dyn}}$ which are listed in Table 3. Several of these galaxies have very high mass to light ratios as discussed below, while others have rather modest values with $M_{dyn}/L_B \sim 1$ in solar units. The highest M_{dyn}/L_B values are found for VCC 405 and VCC 2062, which we conclude in §3.5 are likely not dwarf ellipticals or real detections. We also discuss alternative processes that can potentially create large HI velocity widths besides deep gravitational potential wells.

3.4. New Detections

In this section we discuss the 21-cm and optical properties for each of our new Arecibo HI detections and give some possible interpretations of their measurements. We wish to stress that both of these detections have only occured with Arecibo and its large beam, and confusion with other galaxies could be an issue (Hibbard & Sansom 2003).

3.4.1. VCC 390

In the DSS and WIYN images (Figures 2 and 3) VCC 390 appears as a small compact galaxy. Using the WIYN image of this galaxy (Figure 3) its scale length is fit as 0.29±0.003 kpc (Table 4). This object is classified as a dE3 in the VCC and has an absolute magnitude of $M_B = -14.4$, has low asymmetry, low concentration, and low clumpiness values (Table 4), all consistent with it being a dwarf elliptical (Conselice 2003). It is also fairly well fit by an exponential profile with a Sérsic index, n = 0.95±0.01. This galaxy is however fainter towards its outer parts than its Sérsic fit.

The observed wavelength of the HI line for VCC 390 gives a heliocentric radial velocity of 2400±10 km s^{-1} (Figure 1), in relatively good agreement with its optical radial velocity, 2479±38 km s^{-1} computed though cross-correlation fits of absorption features in the optical VCC 390 spectrum shown in Figure 4. This is a WIYN Hydra Multi-Object Spectrograph (MOS) spectrum taken in April 1999 as part of a radial velocity survey (Paper I). This is a typical early-type galaxy spectrum showing absorption features such as the Mgb triplet at 5175 Å. No emission lines are seen; these would be an indication of active star formation, as seen in Virgo dwarf irregular galaxies (e.g., Gallagher & Hunter 1989; Heller et al. 1999). The spectrum of VCC 390 is also similar to spectra of other Virgo dwarf ellipticals (see Paper I).

The HI line of VCC 390 presents an interesting puzzle due to its large velocity width (Table 3). The 20% and 50% FWHM velocities are 286±5 km s^{-1} and 285±7 km s^{-1} with a total integrated HI flux of 0.8±0.01 Jy km s^{-1}. It is only one of three galaxies in our sample that has a velocity width > 200 km s^{-1}. Due to its faint magnitude, it also has an inferred high dynamical mass to light ratio (M_{dyn}/L_B) of ∼45 in solar units (Table 3). However, it is possible that some of this line emission originates from contamination in the side-lobes due to the nearby galaxy NGC 4277, which is at a velocity 2504 km s^{-1} , and has an HI line profile that overlaps in velocity with VCC 390's (see van Driel et al. 2000). We investigated this possibility by overlaying the Arecibo beam map onto a DSS image of VCC 390 and NGC 4277. We found that the outer lobes of the profile as centered on VCC 390 slightly overlapped with NGC 4277. Short of this, the large velocity width could be the result of gas stripping. It is however impossible to determine using our current data how much these sources are contributing to the VCC 390 signal. Understanding this will require mapping the spatial extent of the HI distribution of VCC 390 and comparing it with that of NGC 4277.

3.4.2. VCC 1713

The other low-mass galaxy with a new HI detection is VCC 1713. Compared to VCC 390, VCC 1713 has a narrower velocity HI profile, with W_{50} = 46±8 km s^{-1} and W_{20} = 60±6 km s^{-1}, more commonly expected for a low-mass galaxy. The total HI flux is slightly higher than that of VCC 390, with an integrated value of 1.1 Jy km s^{-1}, giving a total HI gas mass of 8×10^7 $M_\odot$. Despite its narrow HI line width, this galaxy has a rather bright absolute magnitude of $M_B = -16.2$. This gives a M_{dyn}/L_B value of > 0.4 in solar units.

It is also listed as an uncertain member of the Virgo cluster in the VCC; however, its velocity of 1655 km s^{-1} (Grogin et al. 1998) is consistent with cluster membership. The morphological appearance (Figure 2 & 3) and quantitative morphology of this galaxy suggests that it is a dwarf elliptical-like object (Table 4), with low asymmetry and concentration values. The clumpiness index S is moderately high suggesting the presence of some low level of star formation. There are however no measured colors for VCC 1713, which if it were very blue would qualify as a dwarf irregular object. This object is our best candidate for being an object in an ongoing early transition phase between a star-forming and quiescent LMCG.

3.5. Previous Detections

The seven following objects, all classified as dEs, were previously detected in HI. In some cases we also discuss the possibility that some of these objects are not early-type LMCGs, but are misclassified star-forming galaxies, or spurious HI detections.

3.5.1. VCC 31

VCC 31 has a magnitude of $M_B = -16.4$ and was detected in HI using the Arecibo telescope by van Zee, Haynes & Giovanneli (1995) and at Nançay by van Driel et al. (2000). Van Zee et al. (1995) determined that this galaxy does not have an extended HI distribution, and has a M_{HI}/L_B value high enough to be considered a compact dwarf. Van Driel et al. (2000) also detected this object in HI, although they find a much higher W_{20} value (312 km s^{-1}) than van Zee et al. (1995) (132 km s^{-1}). This indicates that VCC 31 may have extended gas, as the velocity width and flux of the Nançay observations are much larger than the Arecibo results, which used a smaller $3.5'$ beam. There are also no nearby galaxies that would have confused the Nançay results, further suggesting that there is extended HI gas around VCC 31. This galaxy appears symmetric and dwarf elliptical-like on the DSS and WIYN images (Figure 2 and 3). Its quantitative morphology (Table 4) is also consistent with a dwarf elliptical classification. Using the van Zee et al. (1995) parameters of the HI line for this galaxy, we find a M_{dyn}/L_B ratio ~ 2.4 in solar units, while the van Driel et al. (2000) values give ratios a factor of ~ 5 higher.

3.5.2. VCC 168

VCC 168 was first detected in HI using Arecibo by Hoffman et al. (1987), who classified this object as a dE2 or ImIV based on the VCC. This object was later classified by Binggeli & Cameron (1993) as a true dE2. It is not visible on the DSS images (Figure 2), but clearly appears as a dwarf elliptical-like object on the WIYN image, with a quantitative morphology consistent with this interpretation (Table 4) including a light profile well fit by an exponential (Table 4; Figure 3). Heller et al. (1999) searched for Hα in VCC 168, but found none. VCC 168 is also symmetric, with little internal structure, based on its image in Heller et al. (1999) and in Figure 3, implying that the dwarf elliptical classification is the correct one.[7] Almoznino & Brosch (1998) observed VCC 168 in BVR, finding a color $(B-V) = 0.76 \pm 0.17$, the reddest $(B-V)$ color in their sample. This suggests an older stellar population, >2 Gyr since the cessation of significant star formation. This is the case even if the stars are metal rich (Worthey 1994); VCC 168 thus appears to be a quiescent LMCG with gas. Its HI mass of 3×10^7 $M_\odot$ is unusually high for such as faint dwarf

[7] Heller et al. only find five objects out of 43 without Hα emission in their survey of Virgo cluster irregulars, one of which is VCC 168. This further suggests that this object is not a true irregular. The irregular classification of VCC 168 by Heller et al. is solely based on its HI detection by Hoffman et al. (1987).

elliptical. It also has an HI line width of $W_{20} = 64$ km s^{-1} suggesting a dynamical mass to light ratio of $M_{dyn}/L_B \sim 2.5$ (Table 3).

3.5.3. VCC 405

VCC 405 is the faintest object in our HI detected sample with B $\sim$ 20 (VCC) or $M_B \sim -11.5$, and it does not appear on DSS images (Figure 2). This object was marginally detected with Arecibo at 21-cm (Duprie & Schneider 1996) with a single observation, and thus the detection could be spurious. Based on their HI spectrum and the very unlikely physical parameters derived from its HI profile (Table 3), we conclude that this object is indeed probably a false HI detection, and do not consider it in our subsequent analysis.

3.5.4. VCC 608

VCC 608 (NGC 4323), classified as a dE4, N in the VCC, is the second brightest Virgo dwarf elliptical detected in neutral hydrogen, with $M_B = -16.6$. It was first detected in HI by Huchtmeier & Richter (1986). VCC 608 also has a fairly red color with $(B - V) = 0.87 \pm 0.06$ (de Vaucouleurs et al. 1991), consistent with an old stellar population (see the argument in §3.5.2). Ryden et al. (1999) determined that this galaxy has a mean ellipticity of 0.39 with isophotal fits giving $<a_4/a>$ values consistent with a disky structure. Gavazzi et al. (2001) fit surface photometry in the near-IR H(1.6μ) band, finding a good exponential fit, and a low concentration of light, further confirmation that this is morphologically similar to a dwarf galaxy. VCC 608 also has a M_{dyn}/L_B ratio $\sim$ 2.5, based on its HI line width. It also contains a high HI gas content of $\sim 10^9$ $M_\odot$, and has one of the highest HI gas mass fractions in our sample (Table 3).

3.5.5. VCC 797

VCC 797 with $W_{50} = 28$ km s^{-1} has the narrowest HI line of any galaxy in our sample, and the smallest optical scale length of 0.24 kpc. The internal velocity dispersion is low, indicating that its observed HI velocity width may be dominated by turbulence. It is also the only low-mass galaxy that is near a giant galaxy, in this case about $3'$ south of M85 (Figure 2). HI in VCC 797 was discovered by Burstein, Krumm & Salpeter (1987), who detected it during 21-cm observations of M85. Due to the presence of HI, Burstein et al. (1987) considered VCC 797 to be a dwarf irregular, although it is classified as a dE3,N in the VCC. The VCC classification is based on higher resolution images than those available to Burstein et al. (1987). Burstein et al. (1987) however only marginally detect the object at a 4σ level of significance. We tentatively consider this to be a HI detected dE, and not a spurious signal, although this should be confirmed by observing it again at 21-cm with higher sensitivity.

3.5.6. VCC 1949

VCC 1949 is the brightest galaxy ($M_B = -17.1$) in our sample, and it appears as an early-type dwarf on DSS images (Figure 2). It was classified as a dSBO(4),N or dE(6,4),N in the VCC[8]. It was first detected in HI by Huchtmeier & Richter (1986), and later re-observed at 21-cm by Haynes & Giovanelli (1986). The optical image of this galaxy is well fit by an exponential profile (Binggeli & Cameron 1993). VCC 1949 is one of three galaxies in the present sample with very large (> 250 km s^{-1}) inferred HI velocity widths (Table 3), giving it a high measured dynamical mass to light ratio of $M_{dyn}/L_B \sim 20$ in solar units.

3.5.7. VCC 2062

VCC 2062 has been studied previously in HI by both Hoffman et al. (1993) and van Driel & van Woerden (1989). It is about 2 kpc (0.4 arcmin) away from the irregular galaxy NGC 4694, with which it may be interacting. VCC 2062 was classified as a dE in the VCC, although the DSS image in Hoffman et al. (1993) suggests that this classification is incorrect, and that the galaxy is more likely an irregular. Hoffmann et al. also found very blue colors for this object, with $(B-V) = 0.35$ and $(V-R) = 0.19$. These colors indicate that star formation has recently occurred, as an extremely metal poor stellar population which can also produce blue colors, would have to be less than 700 Myrs old to produce these colors (Worthey 1994). The presence of young stars reveals that this object is probably not a classical dE (i.e., old stars and no gas), despite its classification in the VCC.

Due to its fairly high M_{HI}/L_B ratio of ~ 55 this object is also by far the most gas rich member of our sample. The high M_{HI}/L_B ratio exceeds that of typical values found for blue compact dwarf galaxies (van Zee et al. 1995) and irregular galaxies (e.g,. Roberts & Haynes 1994), another indication that it may be an interacting system.

In summary, we conclude that 7 of the 9 detections of HI in LMCGs are genuine, and

[8]Bingelli & Cameron (1993) list VCC 1949 as a dS0.

reject as spurious the HI dE detection claims for VCC 405 and VCC 2062.

4. Interpretations

4.1. Incorrect Morphological Identifications

Although the galaxies discussed in this paper are classified as dEs in the VCC, other studies have given different classifications for a few of these objects, mostly the dwarf irregular class. Could all of these HI detected LMCGs in our sample be misclassified dwarf irregulars? To some degree the problem is semantic assuming that the VCC used a consistent classification approach throughout the Virgo cluster. The identification in the VCC of a dE therefore may be biased, but as long as this bias is consistently applied throughout, then the VCC classified 'dEs' should represent a homogeneous population equally distributed across the cluster.

We also reject the incorrect morphological identification explanation for the following reasons. The qualitative and quantitative morphologies for these objects, as seen in the DSS frames and in the WIYN images, suggest quiescent systems, with no obvious evidence for star formation, with the possible exception of VCC 1713. The available colors for VCC 168 (§3.5.2) and VCC 608 (§3.5.4) also demonstrate that some HI detected early-type LMCGs potentially have older dE-like stellar populations. The HI gas contents for these systems are also too low for these objects to be misclassified normal dwarf irregulars, as Virgo dIrrs have higher HI gas masses and fluxes than those listed in Table 3 (e.g., Hoffman et al. 1987; Gallagher & Hunter 1989; see also Table 5). Therefore we conclude that these HI detected LMCGs are probably not misclassified dwarf irregulars, with the one exception being VCC 2062 which is not included in the following analyses.

4.2. Patterns of HI Depletion and Orbital Structure

In Figures 5 and 6 we show the spatial pattern of HI depletion of Virgo classified dwarf elliptical galaxies, where in Figure 5 galaxies with HI detections are plotted as large filled circles and non HI-detections as open triangles. All of the LMCGs classified as dEs with HI detections are projected towards the outer parts of the cluster. This is quantitatively shown in Figure 6, which plots the fraction of LMCGs classified as dEs with HI detections as a function of projected distance from the luminosity weighted center of the Virgo cluster, as defined by Sandage et al. (1985). Within a projected distance of 0.5 Mpc of the center, the lower limit to the true 3-dimensional distance, we find no galaxies classified as dEs with HI detections.

The presence of most of the HI LMCGs in the outer parts of Virgo may help reveal the origin of these objects. One obvious explanation is that these galaxies have just been accreted into the cluster and have not yet crossed the core. The other possibility is that these galaxies have orbits that take them through the core of the cluster and somehow retain or replenish their HI gas. For the purposes of argument we discuss the infall case, and two idealized orbiting scenarios: radial and high angular momentum orbits.

Cosmological models of galaxy clusters show that most cluster members are originally on moderate, or low, angular momentum orbits (e.g., Crone, Evrard, & Richstone 1994; Ghigna et al. 1998; Huss, Jain, & Steinmetz 1999). Gas stripping processes are also most effective for galaxies on nearly radial orbits (Vollmer et al. 2001). The survival of HI in low mass cluster galaxies therefore depends on orbital parameters, such that galaxies in more circular orbits that avoid the core are more likely to retain their HI. Signatures of this effect also may be seen in samples of giant galaxies (e.g., Dressler 1986; Solanes et al. 2001) and might also be present in some LMCGs. However, Solanes et al. do not find clear evidence for this behavior in Virgo, possibly as a result of complications associated with interactions with substructure in this cluster (see also Vollmer et al. 2001).

Evidence that our HI LMCGs are on high angular momentum orbits includes the distribution of their radial velocities. The expected signature for galaxies on high angular momentum orbits would be a flat-tip distribution in velocities. Galaxies on radial orbits would have a gaussian distribution peaked at the mean velocity of the cluster. The average velocity of the HI LMCGs is rather large and not centered at the average velocity of the cluster, and the distribution of velocities is non-uniform, different from expectations of both the radial and high angular momentum distribution. Although our distribution is not flat-top, it is clearly not uniformly distributed about the mean cluster velocity. The velocity distribution of the HI rich early-type LMCGs velocity distribution is shown in Figure 7, where the shaded part displays the distribution of the HI detected LMCGs, and the open histograms are the velocity distribution of the non-detections. Although we are in the regime of small number statistics, we can make some arguments based on the data available.

The average velocity of the non HI-detected objects is 1287$\pm$183 km s^{-1}, and the HI-detected objects have an average velocity of 1669$\pm$553 km s^{-1}. The velocity dispersions are very similar with σ = 685 km s^{-1} and 697 km s^{-1} for the non-detected and detected objects, respectively. However, for galaxies at > 1.5 Mpc projected separation from the center of Virgo, the velocity dispersion for the HI LMCGs is 200 km s^{-1} higher than for the LMCGs with non HI detections. A Kolmogorov-Smirnov test reveals a 24% probability that these two distributions are similar. Figure 8 shows the histogram of magnitudes for the HI detected (shaded) and non-detected (open) objects, demonstrating that unlike the radial velocities, the magnitudes of the detected objects are not significantly skewed towards any particular values, although they are on average slightly fainter.

To determine the significance of the $\sim$ 400 km s^{-1} difference in average velocity between the HI detected and non-detected LMCGs we perform a Monte Carlo simulation based on the velocities of dEs in Virgo (Paper I). Using the σ and the mean velocity of dEs from Paper I, we randomly select seven galaxy velocities from this Gaussian distribution, and compute the mean of these seven values. This exercise reveals less than a 1% chance ($\sim 3\sigma$) that the 400 km s^{-1} difference is random. Therefore the fact that the velocities of these HI detected LMCGs are not near the mean cluster velocity of 1064$\pm$34 km s^{-1}, and are found in the outer parts of Virgo, is an indication that a fraction of these HI LMCGs are not on radial orbits and are likely on high angular momentum ones with some velocity substructure induced perhaps by galaxies infalling within groups.

4.3. Gas Stripping, Replenishment and Star Formation

The spatial pattern of LMCGs with detectable HI suggests that gas stripping has occurred through interactions with the intracluster medium (Dressler 1986; Vollmer et al. 2001). Such stripping can happen in a number of ways. The most commonly suggested method is ram-pressure stripping, which can deplete a dwarf rapidly in the inner regions of a cluster, in typically less than 0.1 Gyr (Mori & Burkert 2000) for a CDM like halo, although this depends on the time for shock waves to traverse the galaxy, the form of the galaxy's gravitational potential, and properties of the ICM. A more gradual mass loss also occurs due to Kelvin-Helmholtz instabilities (Nulsen 1982). We examine both of these scenarios below.

4.3.1. Ram-Pressure Stripping

The ram-pressure on a galaxy from the interaction of intracluster gas is given by the equation P = $\rho_{\rm ICM} v_{\perp}^2$, where $v_{\perp}$ is the velocity perpendicular to the plane of a galaxy. The efficiency of gas stripping also depends upon the gravitational potential ϕ of a galaxy, i.e., its ability to hold onto its material. The vertical gravitational acceleration of ISM clouds in a disk galaxy is given by $\partial\phi\ /\ \partial z$. If we define a galaxy's gas surface density as σ, then ram-pressure stripping occurs in the galaxy when

$$\frac{\partial \phi}{\partial z}\sigma < \rho_{\rm ICM} v_\perp^2. \tag{3}$$

Here $\rho_{\rm ICM}$ is the density of the intracluster medium of the Virgo cluster, and $v_\perp$, as before, is the relative velocity perpendicular to the plane of the disk. This formula, first proposed by Gunn & Gott (1972), is found to be a good approximation based on detailed simulations (e.g., Abadi, Moore, & Bower 1999; Vollmer et al. 2001).

To determine the intracluster medium density, $n(r)$, as a function of radius, we use a β model (Cavaliere & Fusco-Femiano 1976), and the parameters for the Virgo cluster given by Vollmer et al. (2001),

$$n(r) = n_0 \left(1 + \frac{r^2}{r_0^2}\right)^{-(3/2)\beta}. \tag{4}$$

In this equation r is the physical distance from the center of the cluster, n_0 is the central ICM gas density, which is $n_0 = 4 \times 10^{-2}$ cm^{-3}, and $r_0 = 13.4$ kpc, and $\beta = 0.5$ for Virgo intracluser gas (Vollmer et al. 2001). By knowing the gas density as a function of radius, the fraction of a galaxy's mass in the gas phase, and the velocity of the gas with respect to the intracluster medium, the minimum mass, $\rm M_{limit}$, a galaxy must have to avoid being stripped of gas by ram-pressure can be computed analytically (Mori & Burkert 2000) for CDM halos. If we assume a gas mass fraction of $\sim 0.1 - 0.3$ for a typical LMCG, we can compute $\rm M_{limit}$ as a function of $v_\perp$ and $n(r)$. Using eq. (4) for the gas density as a function of radius in Virgo, we plot in Figure 9 the mass limit $\rm M_{limit}$ as a function of radius at velocities $v_\perp$ from 250 km s^{-1} to 1250 km s^{-1}. Also plotted on this diagram, as solid points, are the dynamical masses and projected distances from the cluster center for each of the seven LMCGs with confident HI detections. This figure shows that at the relatively large distances of the detected HI LMCGs from the Virgo center, their masses are high enough such that ram-pressure stripping cannot rapidly deplete them of all their gas. Thus we see that high angular momentum orbits in the outer parts of the Virgo cluster could allow slow gas removal from accreted field galaxies.

4.3.2. Kelvin-Helmholtz Instabilities

The interface between the Virgo intracluster medium and the interstellar medium of member galaxies produces a Kelvin-Helmholtz instability which could gradually extract gas from these galaxies, aiding ram-pressure in removing gas. The lower-mass limit for Kelvin-Helmholtz instabilities to be efficient is roughly 10^3 times higher than the ram-pressure stripping limit (Mori & Burkert 2000). It is however unlikely that gas rich LMCGs are being depleted gradually through this process, as we argue below. The mass loss rate induced by Kelvin-Helmholtz instabilities is given by Nulsen (1982) as

$$\dot{M} = \pi R^2 \times n(r) \times v, \tag{5}$$

where R is the radius of the galaxy, v is the velocity of the galaxy relative to the intracluster medium and n(r) is the mass density of the intracluster medium. Using typical values (Table 3) of $R = 1$ kpc and $v = 500$ km s^{-1}, we find that $\dot{M} \sim 10^3$ M$_\odot$ Myr^{-1}. The time-scale for gas depletion of a typical LMCG via Kelvin-Helmholtz instabilities is then $\sim\ 10\ -\ 15$ Gyr.

If a small galaxy entered the Virgo cluster sometime in the last few Gyr on a high angular momentum orbit, then it would not yet have been stripped of all its gas, either through ram-pressure or Kelvin-Helmholtz instabilities. Both of these processes are occurring, but they are slowly removing gas from galaxies on high angular momentum orbits in the outer parts of the Virgo cluster. On the other hand, it appears that these galaxies would have been completely stripped of all their gas if they had existed within the cluster on the order of a Hubble time, no matter what their orbits are. The above arguments again suggest that these HI LMCGs are objects that must have recently entered the cluster in the last few Gyr, or have just been accreted.

4.3.3. Gas Replenishment

During the normal course of stellar evolution stars in galaxies will deposit gas into the interstellar medium, thereby increasing the presence of HI. Gas is returned to the ISM from mass loss in stars during the AGB and planetary nebula phases. The amounts returned vary, depending on the age and total mass of the stellar populations (e.g., Faber & Gallagher 1976). Following the arguments in Faber & Gallagher (1976) for giant ellipticals and Gnedin et al. (2002) for the globular cluster ω Centauri, we calculate that the mass returned to the ISM for a LMCG with a stellar mass of $\sim 10^8$ M$_\odot$ is $\sim 10^6$ M$_\odot$ Gyr^{-1}. If we assume that the HI LMCGs have been in the cluster for a few Gyr, then not enough time has elapsed to produce the observed HI gas content of the HI detected early-type LMCGs from evolved stars. However, if this was the complete story, we might expect substantial HI content to be a common feature of very old early-type LMCGs, but we see very little HI in field ellipticals galaxies or in low-mass cluster galaxies (e.g., Knapp, Kerr & Bowers

1978; Young & Lo 1997; Sage, Welch & Mitchell 1998). It is still not known with certainty why giant elliptical galaxies are depleted of cold interstellar gas, but what ever the cause of depletion, it is likely occurring in LMCGs as well. In summary, we do not consider the return of gas from stellar evolution a likely scenario to explain the HI gas content of these HI LMCGs.

4.3.4. Impulsive Encounters - Dynamical Stripping

The high number density and large relative velocities of cluster galaxies makes impulsive encounters between them common, and can result in mass loss, such as in the harassment scenario (e.g., Moore et al. 1998), although this effect is likely not important for the HI LMCGs since they are located in the outer parts of Virgo. The energy imparted to a galaxy with mass M_{gal} during an impulsive encounter between two spherical galaxies is proportional to $E \alpha M_{pert} M_{gal} b^{-4} V^{-2}$ (Spitzer 1958) where M_{pert} is the mass of the perturbing galaxy, b is the distance between the two galaxies and V is the relative velocity between them. The large separation of the HI LMCGs from the center of Virgo is an indication that the factor b is much larger than for most cluster galaxies. At a typical LMCG impact parameter of of 0.5 - 1 Mpc, the energy imparted to a galaxy and its resulting mass loss due to impulsive encounters is very small (Aguilar & White 1985). The strongest effects of mass loss involve cluster galaxies on nearly radial orbits where the parameter b becomes small (Moore et al. 1998). If the HI LMCGs are on high angular momentum orbits, as has been argued, then they do not feel the strong effects of impulsive encounters and thus will not lose a significant amount of mass from these interactions. This is especially true if the HI LMCGs have only been in the cluster for a short time. We conclude therefore that the only processes strongly affecting the HI LMCGs are ram pressure induced gas loss.

4.4. Morphological Transformations

The question we address in this section is whether or not the HI detected LMCGs have recently been accreted into Virgo (and not yet been stripped of their gas), or if they have been in the cluster for at least a few Gyr, having evolved from a precursor of different morphology. As we argued in §4.2 - 4.3, it is unlikely that these galaxies are an old cluster population. Here we conclude that these LMCGs originate from accreted field populations.

The idea that galaxies can undergo a morphological transformation in clusters has considerable observational support. Distant clusters contain large populations of blue, distorted galaxies (e.g., Oemler, Dressler, & Butcher 1997; Couch et al. 1998), which are not seen in the same proportion in nearby clusters (cf. Conselice & Gallagher 1998, 1999). There is also evidence that S0 galaxies are less common in moderate redshift clusters than in comparison to similar clusters at low redshifts (Dressler et al. 1997). Furthermore, in Paper I we argue that all galaxy types, except giant ellipticals, have kinematic and spatial properties suggesting they were accreted into Virgo after its initial formation, perhaps due to hierarchical accretion into the cluster (Kauffmann 1995). Once they enter the cluster, galaxies can morphologically evolve into earlier types (Moore et al. 1998; Mao & Mo 1998; Abadi et al. 1999; Quilis et al. 2000). What is missing from these arguments is whether or not galaxies in nearby clusters are undergoing evolution, or morphological transformations, as they should if any are still being accreted into clusters, albeit at reduced rates compared to clusters at high redshift (e.g., Tully & Shaya 1984). Previous observations suggest that there are some small galaxies in the Virgo cluster that appear to be undergoing rapid evolution (Gallagher & Hunter 1989; Vigroux et al. 1996), but the extent of this process is currently unknown. Does most active evolution of cluster galaxies, including morphological transformations, occur only in the distant past? We argue here that HI LMCGs are possible examples of objects slowly undergoing transformations today. The evidence, which we discuss in detail below, includes: the outer spatial distribution of these detections in Virgo, their mixed morphological appearances, their gas and stellar content, and the correlation between HI line-width and total B-band magnitude.

4.4.1. Morphologies and Stellar Populations: Dwarf Elliptical-Like

We can try to understand when and how stars in HI detected LMCGs formed by examining their morphologies and the limited spectral information we have. The morphologies and structural parameters of these galaxies (Figure 2-3, Table 4) are clearly not influenced by star formation. The red colors of VCC 168 and VCC 608 demonstrate that these objects contain older stellar populations, and the clumpiness parameter S is low enough that any star formation in these HI LMCGs must be smoothed out. The question is, how long does it take for a young stellar population to become this red and smooth? A galaxy's stellar populations will be smoothed out after approximately a crossing time when young stars die and the population dissolves into the background (Harris et al. 2001) which takes a few Gyr for these galaxies, especially if their random motions are increased slightly through dynamical heating (Moore et al. 1998). For a stellar population to become as red as VCC 168 and VCC 608 from a blue star-forming irregular, or disk galaxy, requires roughly the same amount of time. These HI detected LMCGs therefore have stellar population and morphological characteristics of dwarf ellipticals, and must have had their last major episode of star formation several Gyr ago.

4.4.2. Gas Content: Dwarf Irregular-Like

A diagnostic for understanding the origin of HI-detected LMCGs is to compare their optical and HI properties, including M_{HI}/L_B values, absolute magnitudes and HI masses, to those of other galaxy populations, including the Gallagher & Hunter (1989) Virgo cluster dwarf irregular and amorphous samples. Table 5 lists the averages of several of these quantities as a function of galaxy type. The HI gas mass fractions and M_{HI}/L_B ratios are fairly similar in the various galaxy populations, except for the Local Group dEs, where these values are significantly lower. Dwarf irregulars in the Local Group have the highest f_{gas} and M_{HI}/L_B ratios, while the Local Group dEs have the lowest.

For example, the gas mass fraction, f_{gas}, for dwarf irregulars in the Local Group are 0.07, 0.08, 0.2, 0.65 and 0.46 for the Large Magellanic Cloud, NGC 6822, IC 10, IC 1613 and DDO 221. The average f_{gas} value for all Local Group dwarf irregulars is 0.30±0.24 (Table 5). Virgo LMCGs classified as dEs with HI detections in Virgo have an average f_{gas} value of 0.30±0.28 (Table 3). On the other hand, the gas mass fractions for Local Group dwarf spheroidals are often $< 10^{-4}$ - $10^{-5} \sim 0$ (Johnson & Gottesman 1983; Koribalski et al. 1994; Young & Lo 1997; Young 1999).

Some M_{HI}/L_B values for the HI detected LMCGs are as high or higher than some spirals and irregulars, although some gas rich low-luminosity early types have been found (Sadler et al. 2000). Even if some gas mass is lost through various stripping effects, the fading of stellar populations due to the truncation of star formation (§4.4.4) may be able to reproduce this. Stellar populations with initial colors similar to late-type spirals and irregulars will become ~ 1.5 magnitudes fainter in ~ 3 Gyr, easily allowing for high M_{HI}/L_B values even if some gas is removed. Some of these systems could also be low M_{HI} accreted field galaxies, as some examples are known to exist in the field (Knezek, Sembach & Gallagher 1999).

Average values of other properties, listed in Table 5, show that Local Group dwarf ellipticals/spheroidals have very different derived HI gas properties from the Virgo HI detected LMCGs classified as dEs. In fact, the average values are different at a 7σ significance. Based on this, the HI dEs cannot simply be recently accreted analogs of Local Group dwarf ellipticals/spheroidals, as they have too much HI. Although the HI detected LMCGs studied here morphologically appear to be dwarf ellipticals, they could not have originated from dEs in groups, as no pure dwarf elliptical has a gas content as large as these LMCGs. We propose that the only way these galaxies could contain such a high HI gas mass is for them to have originally been star-forming systems that morphologically evolved into a dE-like object over the last few Gyr through slow gas removal and passive evolution. The most similar galaxy type to the Virgo HI detected LMCGs are the Local Group transition types, Phoenix and Pisces, and irregulars, which have f_{gas} and M_{HI}/L_B values within 1σ of the LMCG values (Figure 10), although the HI masses for these LMCGs are more similar to the values found for the irregulars. As we argue in §4.4.4, star formation in these systems could be suppressed.

4.4.3. Parameter Space: Transition Types

We can further use diagnostic plots such as Figures 10 through 13 to understand which of the well-understood nearby galaxy populations is most similar to the HI LMCGs. Figure 10 plots f_{gas} and M_{HI}/L_B values for individual Local Group spirals (open boxes), irregulars (open triangles), dEs (solid triangles), transition types (crosses) and the Virgo HI LMCGs studied in this paper (solid circles). The average f_{gas} and M_{HI}/L_B values for each type are labeled by a circled small version of their respective identification symbol, and the average values are listed in Table 5. Again, from this figure it appears that the HI detected LMCGs are most similar to the Local Group transition types in terms of their HI gas and stellar properties.

We can also examine the differences between the Virgo dEs with HI compared to Virgo cluster dwarf irregulars observed by Gallagher & Hunter (1986, 1989). Figure 11 plots M_{HI}/L_B ratios vs. M_B for the HI LMCGs, nearby dwarf transition types, and the dwarf irregular and amorphous galaxies studied by Gallagher & Hunter (1989), converted to our assumed distance of 18 Mpc. Figure 11 includes the Virgo amorphous galaxies, objects that morphologically appear to be early-types but have evidence for star formation (Sandage & Brucato 1979). Figure 11 shows that the Virgo LMCGs classified as dEs with HI detections (solid circles) on average have M_{HI}/L_B values between the values found for the gas rich Virgo irregulars and the amorphous galaxies, which are gas depleted (see Table 5). The nearby dwarf transition types in the Local Group are plotted as crosses on Figure 11 and their M_{HI}/L_B distribution is very similar to the M_{HI}/L_B ratios for HI LMCGs classified as dEs.

4.4.4. The Four LMCG Populations (Yet Known)

We can gain further insight into LMCGs by examining the limited information we have on the stellar and gaseous properties of all the different types. Figure 12 shows the correlation between the $(U-B)$ colors and the M_{HI}/L_B ratios of the Virgo dwarf irregular and amorphous samples from Gallagher & Hunter (1989). As Figure 12 shows, the more gas-depleted objects, as measured by the M_{HI}/L_B ratio, have redder $(U-B)$ colors, indicating the increasing dominance of older and possibly more metal rich stellar populations. We also plot on Figure 12 the location of the two HI LMCGs with $(B-V)$ color measurements, VCC 168 and VCC 608. We convert the $(B-V)$ colors for these objects into a $(U-B)$ color by fitting, and using, the relationship between these two colors for all galaxies in the RC3: $(U-B) = 1.26 \pm 0.01\ (B-V) - 0.71 \pm 0.01$. The HI detected LMCGs have M_{HI}/L_B values similar to Virgo dwarf irregulars, but have red colors, similar to the amorphous galaxies. It appears that these HI LMCGs are members of a new class of LMCGs. An arrow on Figure 12 shows where dEs with no detectable HI would fall on this diagram, as they are red and gas depleted systems.

Based on this there appear to be at least four types of low-mass galaxies associated with the Virgo cluster: 1. the classical dwarf irregulars with active star formation and gas, which are likely in the process of being accreted into clusters (Gallagher & Hunter 1989; Paper I); 2. dwarf ellipticals with older stellar populations and HI gas masses $< 10^6$ $M_\odot$ that were accreted $>$ 3 Gyr ago, some as larger mass galaxies, or those that originally formed with the cluster (Paper III); 3. amorphous galaxies; and 4. the HI rich early-type LMCGs studied in this paper. These last two types are likely LMCGs undergoing morphological evolution from accreted low-luminosity disks or irregulars. The amorphous galaxies, because of their low HI content, and red colors, are possibly systems that were accreted into eccentric orbits, or under physical conditions such as within groups, where they lost a significant amount of their HI gas mass. HI LMCGs, discussed in this paper, are potentially dEs which may have retained their HI gas because they were accreted into the cluster on high angular momentum orbits. The redder colors of VCC 168 and VCC 608, and the morphologies of the HI LMCGs, both suggest that HI LMCGs have existed in the cluster for a longer time than the amorphous galaxies.

In the above picture we are not arguing that all dwarf ellipticals originate from dwarf irregulars, as the usual objections for this evolutionary process still hold (Paper I). The only dwarf ellipticals/spheroids that originate from the irregulars would be those that are faint with low surface brightnesses. The origin of the brighter, higher surface brightness objects is potentially dynamical in nature (Paper I and III, Conselice 2002).

4.5. The Luminosity-Line Width Relationship

Figure 13 shows the luminosity line width diagram for the HI LMCGs detections listed in Table 3, minus the two galaxies we conclude are either not likely a dE or a false HI detection. With the exception of VCC 390, which has a high M_{dyn}/L_B ratio of $\sim$45, there is a general correlation between the absolute magnitude M_B and the velocity width W_{20}. Also plotted on Figure 13 are the Faber-Jackson and Tully-Fisher relationships between M_B and the velocity line width, or internal stellar velocity dispersion. Data from which these relationships are fitted are shown, and are from Faber & Jackson (1976) and Pierce & Tully (1992)[9]. Also plotted in Figure 13, as crosses, are very late-type disk galaxies, which are good candidates for being LMCG progenitors, taken from Matthews et al. (1998).

The magnitude and velocity data for the HI LMCGs listed Table 3 are plotted as open circles, and represent the magnitudes and W_{20} values after correcting for inclination and subtracting out a component to account for turbulence. While the turbulent velocity contribution could be fairly high in some galaxies (Tully & Fouqué 1985; de Blok, McGaugh & van der Hulst 1996), it is likely lower in dwarfs, $\sim$5 km s^{-1} based on measurements of nearby low-mass galaxies (e.g., Young & Lo 1997). We therefore remove 5 km s^{-1} from the W_{20} velocity widths when correcting for turbulence.

The solid line shows a best fit relationship between the galactic extinction corrected M_B values and velocity widths for the HI LMCGs. This fit shows that the LMCGs classified as dEs with HI gas appear to deviate from the Tully-Fisher and Faber-Jackson relationships in both slope and zero point, and are more similar to the trends, shallower slope, and individual values found for the extreme late-types in the Matthews et al. (1998) sample. This relationship is also fairly flat and several galaxies clearly deviate from it. Figure 13 shows that the galaxy sample under consideration, while displaying a luminosity line-width correlation on average (solid line), has a fundamentally different nature than the relationship for both the spirals and ellipticals. While e.g., Matthews et al. (1998) find that some faint galaxies have high velocities for their magnitudes compared to Tully-Fisher, revealing a possible high mass to light ratio, we do not generally see this trend for all the HI detected LMCGs.

There are several possible ways to account for the dispersion in the relationship between HI line width and absolute magnitude in the HI detected early-type LMCGs,

[9] We convert the magnitudes in Faber & Jackson's (1976) photometry to match the Hubble constant, 85 km s^{-1} Mpc^{-1} used in Pierce & Tully (1992). The magnitudes for the spiral galaxies in Pierce & Tully (1992) were corrected for internal and galactic extinction. The velocity widths, W_R, plotted for the spiral data are corrected using the methods outlined in Tully & Fouqué (1985).

besides observational error. One is that these galaxies are in a mix of evolutionary stages, such that the velocity width is sensitive to not only the mass of the galaxy, but also whether or not the gas disk has been extended or truncated by cluster processes such as gas and tidal stripping (Moore et al. 1998). Models of the evolution of low-mass galaxies in groups also show that as a galaxy interacts with a larger system and losses mass, its mass to light ratio varies with time depending on whether any new star formation occurs, and what the mass profiles of the various components are (e.g., Mayer et al. 2001). The mass to light ratio could also be somewhat overestimated by the material stripped from galaxies that can produce a larger observed velocity dispersion, and a range of derived M/L ratios (Mayer et al. 2001). This would however require non-virial motions of the gas, that are unlikely if ram-pressure forces are reduced in intensity (§4.3).

5. The Recent Virgo Accretion Rate

We can use the information on the number of transition type dwarfs in the Virgo cluster to get an idea of the recent galaxy accretion rate which might be responsible for producing these objects. In this section we follow the basic outline presented by us in Gallagher et al. (2001). First we assume that the total number of dwarf spheroidal/ellipticals in a cluster, $N_{dE}(t)$, can be increased or decreased due to formation and destruction processes in a simple one spatial zone model. In what follows, we also ignore mass-dependent effects, any possible non-linearities, such as a quadratic destruction rate based on the total number of LMCGs, and only examine the gross evolution of moderate luminosity dEs with $M_V \leq -14$. We take a general approach to this problem below to show how dwarf formation/destruction can be approached in a rigorous way, although our final result can be obtained through a simpler analysis.

We define $P_{dE}(t)$ as the production rate of new dE systems at time t and $D_{dE}(t)$ as the destruction rate, then the rate of increase or decrease in the dE population is given by $\dot{N}_{dE}(t) = P_{dE}(t) - D_{dE}(t)$. If the cluster formed at t_f, then the number of dEs at the current time t_0 is

$$N_{dE}(t_0) = N_{dE}(t_f) + \int_{t_f}^{t_0} \dot{N}_{dE}(t)dt.$$

For a purely primordial cluster dE population we require $P_{dE}(t) = D_{dE}(t) = 0$ at all t, which is physically unlikely. However, we might expect that dEs are produced from galaxies accreted into clusters, e.g., as in the models of Moore et al. (1998; see also Quilis et al. 2000). Then for an infall rate $\dot{N}_c(t)$, we can express the production rate by $P_{dE}(t) = c_{dE}(t)\dot{N}_c(t)$, where $c_{dE}(t)$ is the efficiency of conversion of accreted galaxies into dEs. The destruction rate would also depend upon a destruction efficiency, $d_{dE}(t)$, such that $D_{dE}(t) = d_{dE}(t)N_{dE}(t)$, although in what follows we assume no destruction, $d_{dE}(t) = 0$.

If all dEs formed from accreted systems then $N_{dE}(t_f) = 0$, we can estimate a minimum average infall rate over the life of the cluster by setting $d_{dE}(t) = 0$ for all t,

$$\overline{\dot{N}_c(t)} = N_{dE}(t_0)/\bar{c}_{dE}(t_0 - t_f).$$

If we assume a cluster age of 10 Gyr and a dE production efficiency from all but giant galaxies of 100%, then since there are $\sim 10^3$ dEs in Virgo with $\mathrm{M_B} \leq -14$, this requires an average infall rate of $\geq$100 galaxies per Gyr. High infall rates in the past are therefore necessary to populate modern clusters with low-mass cluster objects, but higher past cluster infall rates are likely in a low Ω_M universe (Kauffmann 1995).

Infall rates are difficult to measure, and probably will be episodic, since galaxies are observed to accrete into Virgo in groups (e.g., Tully & Shaya 1984). One estimate can be derived from the Gallagher & Hunter (1989) sample which suggests that a few dozen galaxies are currently undergoing morphological transformations. This is similar to the $\sim$ 20 galaxies estimated to have recently fallen into Virgo in the last Gyr (Tully & Shaya 1984). We obtain another estimate of the total number of current transition dwarf objects in the Virgo cluster using the results of this paper. A total of 49 objects classified as dwarf ellipticals were observed for HI for which a total of 7 are likely transition objects. If we assume that these 49 are representative of the entire Virgo dwarf elliptical population, and ignore any transition types that may be classified as dwarf irregulars, then $\sim$15% of all dwarf ellipticals with $\mathrm{M_B} < -14$ in the Virgo cluster are in some kind of transition phase. As there are roughly 10^3 dwarf ellipticals in the Virgo cluster (Binggeli et al. 1985), then we expect $\sim$160 of these galaxies to be in transition throughout Virgo. If we assume that an average transition phase takes 1-3 Gyr (e.g., Moore et al. 1998) then the recent galaxy infall rate in the last 3 Gyr (from z$\sim$ 0.2 in ΛCDM) is $\dot{N}_c(t_0) \approx 160$ galaxies / 3 Gyr $\sim$ 50 galaxies/Gyr. This is an upper bound as some mixed structure galaxies could be on nearly circular orbits, and thus slowly evolving.

We can use further assumptions about the average amount of mass per galaxy, to derive a mass infall rate of dwarfs into the Virgo cluster in the last 3 Gyr. The average absolute magnitude for the HI detected LMCGs is $\mathrm{M_B} = -15.6 \pm 1.2$. This gives an average mass per galaxy, assuming a stellar M/L ratio of 5 in solar units, of $\sim 5 \times 10^8$ $\mathrm{M_\odot}$. Using this approximation for our hypothetical 160 transition dwarfs accreted over the last 3 Gyr gives a mass influx into the Virgo cluster of $\sim$ 50 $\mathrm{M_\odot}$/yr only from this low-mass component. Assuming a normal luminosity function for infalling galaxies the total time average infall rate would be several times larger than this, $\sim 200 - 300$ $\mathrm{M_\odot}$/yr. While we have used a very simplistic model to obtain this result, it shows that an accretion model for HI LMCGs evolving into dwarf ellipticals gives reasonable galaxy and mass infall rates, comparable to other Virgo cluster accretion estimates (e.g., Tully & Shaya 1984).

Are these calculations of the recent and past accretion history into clusters consistent with cosmological model predictions? In a Λ-dominated flat cosmology, the linear growth of structure slows down at intermediate redshift, $1 + z \sim \Omega_m^{-1/3}$ (note this is a lower redshift than that at which linear growth slows for a matter-dominated open universe with the same Ω_m), but growth is a process that continues until the present day, with larger structures assembling a larger fraction of their mass later. Simulations designed to constrain cosmological parameters through the analysis of the amplitude of substructure in clusters (Crone, Evrard & Richstone 1996) have shown that in a model with $\Omega_\Lambda = 0.8$, $\Omega_m = 0.2$ and a power spectrum similar to that of CDM over cluster mass scales ($n = -1$), 50% of the mass of a typical large cluster was assembled within the last 5 h^{-1} Gyr. The ΛCDM simulations of Wechsler et al. (2002) also show continuous accretion and mass assembly to the present day, with their most massive haloes, $M > 3 \times 10^{13} h^{-1} M_\odot$, somewhat lower than a typical galaxy cluster, accreting around 25% of their mass since $z \sim 0.7$ (their Fig. 4a), or a look-back time of $\sim$ 7 Gyr. These haloes accrete typically about 10% of their mass in the last $\sim$ 3 Gyr ($z \sim 0.25$). The 'Virgo-like' clusters simulated by Governato, Ghigna and Moore (2001) also accrete $\sim$ 20% of their mass since $z = 0.25$ in the 'concordance' ΛCDM universe (see their Fig. 5; a similar recent accretion history is found in the open CDM model). These CDM models are therefore consistent with the idea, that Virgo HI rich early-type LMCGs are a recently accreted galaxy population.

6. Summary and Conclusions

In this paper we present evidence that HI-rich Virgo cluster dEs, discovered through an Arecibo 21-cm and WIYN 3.5-m telescope study, form a new class of low-mass galaxies.

1. We find two new low-mass galaxy HI 21-cm line detections with the Arecibo telescope in the Virgo cluster, out of 22 observed objects classified as dEs with optically determined radial velocities. These dwarfs, VCC 390 and VCC 1713, have $M_{HI} = 6 \times 10^7$ $M_\odot$ and 8×10^7 $M_\odot$, respectively. The other 20 Virgo dE members we observed were not detected, with 3σ upper limits of $M_{HI} \leq 8 \times 10^6$ $M_\odot$, corresponding to $M_{HI}/L_B < 0.1$ (see Table 1).

2. A survey of the literature yields an additional 5 Virgo early-type dwarfs with credible HI measurements, for a total of 7 detections among 49 galaxies with sensitive 21-cm

line observations (Table 2). About half of all Virgo dEs with measured radial velocities (see Paper I) now have been searched for HI to the $\sim 10^7$ $M_\odot$ level with a 15% HI detection rate.

3. Optical imaging with the WIYN telescope for 5 of these Virgo early-type LMCGs with 21-cm detections allowed us to perform morphological classifications using quantitative techniques. One of our new detections, VCC 1713, shows clumpy sub-structure, which could be due to internal dust or residual effects of star formation; it appears to be in a relatively early stage of transition from a star forming galaxy to a dE like system. We further suspect that VCC 2062 is a dI galaxy, as it has a faint, patchy structure on DSS images, and we removed it from the early-type Virgo LMCG sample. The morphologies and other known optical structural characteristics of the remaining 5 HI-detected galaxies are consistent with those of normal dE members of the Virgo cluster. The Virgo HI-rich LMCGs have gas masses well above the levels found in Local Group dEs, e.g., NGC 185 and NGC 205. These relatively gas-rich galaxies may constitute $\sim$15% of Virgo's moderate luminosity population of early-type dwarf galaxies.

4. The early-type LMCGs in Virgo with HI are found preferentially near the edge of the cluster, at radii ≥ 0.5 Mpc from the cluster center, and have a flat distribution of observed radial velocities, suggesting that they have recently been accreted (and not crossed the cluster yet), or are on high angular momentum orbits and are possibly accreted in groups.

5. We show that the HI LMCGs studied in this paper have HI properties more similar to Local Group transition type dwarfs or dwarf irregulars, rather than dEs or Virgo amorphous galaxies.

We use this observational information, along with models of various cluster driven galaxy evolutionary processes, especially gas removal due to ram-pressure stripping and Kelvin-Helmholtz instabilities, to conclude the following about these HI LMCGs and other low mass cluster galaxies in Virgo.

1. Based on the positions of HI LMCGs in the outskirts of Virgo and their high velocities relative to the cluster, we conclude that some, or all, of the HI-rich Virgo dEs are on high angular momentum orbits, and therefore never go through the cluster core. This is a natural explanation for how these galaxies are able to keep their HI gas over long time spans. If these galaxies had highly eccentric orbits, and passed through the Virgo center, they would be rapidly stripped of their gas in less than a cluster crossing time.

Calculations of gas loss due to ram-pressure and Kelvin-Helmholtz instabilities show that these galaxies would be depleted of HI gas, even at their projected position, over $\sim$ 10 Gyr, but can potentially keep their gas when on high angular momentum orbits for up to a few Gyr.

2. Through a comparison of gas properties of Local Group dwarf ellipticals and spheroidals, which have much lower gas content than the Virgo HI-rich LMCGs classified as dEs, we conclude that these galaxies must have been of a different morphological type in the past. This is consistent with the idea that these galaxies were accreted as gas rich star-forming systems into Virgo during the last 1 - 3 Gyr, as this is approximately the same amount of time needed to convert a disk or irregular galaxy with star formation into a red early-type dwarf. Even at the present epoch, galaxy clusters act as engines of evolutionary change. They effectively strip gas and stars from later-type low mass galaxies captured from the cluster surroundings, and thereby could convert low luminosity disk galaxies and irregulars into early-type cluster dwarfs.

3. Combining this analysis with the dwarf irregular and amorphous galaxy properties from Gallagher & Hunter (1989), and Paper I, we can sketch a possible evolutionary/formation scenario for low-mass cluster galaxies in Virgo. The dwarf irregulars are recent additions into clusters that have not yet crossed through the cluster, but when they do they will be stripped of much of their gas. The presence of HI in some Virgo LMCGs classified as dEs is additional evidence that some LMCGs are created from infalling field galaxies (Paper I & III). Other dwarf ellipticals in Virgo have likely been present since the cluster was formed. We argue that the amorphous and HI LMCGs are both accreted populations, either former disk galaxies or dwarf irregulars, whose evolution has diverged due to their orbits in the cluster. The amorphous galaxies are possibly on radial orbits, or systems in previous collisions (Gallagher & Hunter 1989), whose HI gas has been stripped, and are now passively evolving into redder systems. The HI LMCGs are, in our scenario, systems on circular orbits whose HI gas remains, and whose stellar populations and morphologies evolved to resemble dwarf ellipticals. In this model, the HI LMCGs were accreted before the amorphous galaxies to allow time for morphological evolution.

4. A simple calculation of expected Virgo cluster infall rates based on the number of low-mass galaxies observed in evolutionary transition phases yields reasonable results, with a derived recent infall rate of $\dot{\mathrm{M}} \sim 50\ \mathrm{M}_\odot\ \mathrm{year}^{-1}$, and most likely a time averaged rate of 200 - 300 $\mathrm{M}_\odot\ \mathrm{year}^{-1}$, when giant galaxies are included.

We thank Chris Salter for his invaluable assistance in obtaining the data presented in this paper, and for his generous hospitality while CJC was observing at Arecibo. We also thank Lynn Matthews for help taking the WIYN images, and for supplying us with velocities and magnitudes of her low-mass disk galaxy sample. The anonymous referee made many valuable points after a careful and thorough reading of this paper. This research was supported in part by the National Science Foundation (NSF) through grants AST-9803018 to the University of Wisconsin-Madison and AST-9804706 to Johns Hopkins University. CJC acknowledges support from a NSF Astronomy & Astrophysics Postdoctoral Fellowship, a Grant-In-Aid of Research from Sigma Xi and the National Academy of Sciences (NAS) as well as a Graduate Student Researchers Program (GSRP) Fellowship from NASA and the Graduate Student Program at the Space Telescope Science Institute.

REFERENCES

Abadi, M.G., Moore, B., & Bower, R.G. 1999, MNRAS, 308, 947

Aguilar, L.A., & White, S.D.M. 1985, ApJ, 295, 374

Almoznino, E., & Brosch, N. 1998, MNRAS, 298, 920

Baars, J.W.M., Genzel, R., Pauliny-Toth, I.I.K., & Witzel, A. 1977, A&A, 61, 99

Bershady, M.A., Jagren, A., & Conselice, C.J. 2000, AJ, 119, 2645

Binggeli, B., & Cameron, L.M. 1993, A&AS, 98, 297

Binggeli, B., Tammann, G.A., & Sandage, A. 1985, AJ, 94, 251

Blumenthal, G.R., Faber, S.M., Primack, J.R., & Rees, M.J. 1984, Nauture, 311, 517

Bothun, G.D., Mould, J.R., Wirth, A., & Caldwell, N. 1985, AJ, 90, 697

Broeils, A.H. 1992, PhD Thesis, Univ. Groningen

Burstein, D., Krumm, N., & Salpeter, E.E. 1987, AJ, 94, 883

Cavaliere, A. & Fusco-Fermiano, R. 1976, A&A, 49, 137

Conselice, C.J. 1997, PASP, 109, 1251

Conselice, C.J., & Gallagher, J.S. 1998, MNRAS, 297, 34L

Conselice, C.J., & Gallagher, J.S. 1999, AJ, 117, 75

Conselice, C.J., Gallagher, J.S., Wyse, R.F.G. 2001a, ApJ, 559, 791 (Paper I)

Conselice, C.J., Gallagher, J.S., Wyse, R.F.G. 2001b, AJ, 122, 2281

Conselice, C.J., Gallagher, J.S., Wyse, R.F.G. 2002, AJ, 123, 2246 (Paper II)

Conselice, C.J., Gallagher, J.S., Wyse, R.F.G. 2003, AJ, 125, 66 (Paper III)

Conselice, C.J. 2002, ApJ, 573, 5L

Conselice, C.J. 2003, ApJS, in press

Conselice, C.J., Bershady, M.A., & Jangren, A. 2000a, ApJ, 529, 886

Conselice, C.J., Bershady, M.A., & Gallagher, J.S. 2000b, A&A, 354, 21L

Couch, W.J., Barger, A.J., Smail, I., Ellis, R.S., & Sharples, R.M. 1998, ApJ, 497, 188

Crone, M. M., Evrard, A. E., & Richstone, D. O. 1994, ApJ, 434, 402

Dressler, A. 1986, ApJ, 301, 35

Dressler, A., et al. 1997, ApJ, 490, 577

Duprie, K., & Schneider, S.E. 1996, AJ, 112, 937

Ellingson, E., Lin, H., Yee, H.K.C., & Carlberg, R.G. 2001, ApJ, 547, 609

Faber, S.M., & Jackson, R.E. 1976, ApJ, 204, 668

Faber, S.M., & Gallagher, J.S. 1976, ARA&A, 204, 365

Ferguson, H.C. 1989, AJ, 98, 367

Ferguson, H.C., & Binggeli, B. 1994, A&ARv, 6, 67

Ferguson, A.M.N., Wyse, R.F.G., Gallagher, J.S., & Hunter, D.A. 1998, ApJ, 506, 19L

Gallagher, J.S., & Hunter, D.A. 1984, ARA&A, 22, 37

Gallagher, J.S., & Hunter, D.A. 1986, AJ, 92, 5

Gallagher, J.S., & Hunter, D.A. 1989, AJ, 98, 806

Gallagher, J.S., & Wyse, R.F.G. 1994, PASP, 106, 1225

Gallagher, J.S., & Conselice, C.J., & Wyse, R.F.G. 2002, preprint: astro-ph://0108007

Gavazzi, G., Zibetti, S., Boselli, A., Franzetti, P., Scodeggio, M., & Martocchi, S. 2001, A&A, 372, 29

Ghigna, S., Moore, B., Governato, F., Lake, G., Quinn, T., & Stadel, J. 1998, MNRAS, 300, 146

Gnedin, O.Y., Zhao, H., Pringle, J.E., Fall, S.M., Livio, M., & Meylan, G. 2002, ApJ, 568, 23L

Governato, F., Ghigna, S. & Moore, B. 2001, in Astrophysical Ages and Timescales, ASP Conf Ser vol 245, eds T. von Hippel, C. Simpson & N. Manset (ASP, San Francisco) p469 (astro-ph/0105433)

Grogin, N.A., Geller, M.J., & Huchra, J.P. 1998, ApJS, 119, 27

Gunn, J.E., & Gott, J.R. 1972, ApJ, 176, 1

Harris, J., Calzetti, D., Gallagher, J.S., Conselice, C.J., & Smith, D.A. 2001, AJ, 122, 3046

Haynes, M.P., & Giovanelli, R. 1986, ApJ, 306, 466

Heller, A., Almoznino, E., & Brosch, N. 1999, MNRAS, 304, 8

Hibbard, J.E., & Sansom, A.E. 2003, AJ, 125, 667

Hoffman, G.L., Helou, G., Salpeter, E.E., Glosson, J., & Sandage, A. 1987, ApJS, 63, 247

Hoffman, G.L., Lu, N.Y., Salpeter, E.E., Farhat, B., Lamphier, C., & Roos, T. 1993, AJ, 106, 3

Huchtmeier, W.K. 1979, A&A, 75, 170

Huchtmeier, W.K., & Richter, O.-G. 1986, A&AS, 64, 111

Huss, A., Jain, B., & Steinmetz, M. 1999, MNRAS, 308, 1011

Johnson, D.W., & Gottesman, S.T. 1983, ApJ, 275, 549

Kauffmann, G. 1995, MNRAS, 274, 153

Kennicutt, R.C. 1989, ApJ, 344, 685

Knezek, P.M., Sembach, K.R., & Gallagher, J.S. III, 1999, ApJ, 514, 119

Knapp, G.R., Kerr, F.J., & Bowers, P.F. 1978, AJ, 83, 360

Koribalski, B., Johnston, S., & Ortupcek, R. 1994, MNRAS, 270, 43L

Kuehr et al. 1981, A&AS, 45, 367

Lewis, B.M., Helou, G., & Salpeter, E.E. 1985, ApJS, 59, 161

Mao, S., & Mo, H.J. 1998, MNRAS, 296, 847

Martin, C.L., Lotz, J., & Ferguson, H.C. 2000, ApJ, 543, 97

Matthews, L., van Driel, W., & Gallagher, J.S. 1998, AJ, 116, 2196

Mayer, L., Governato, F., Colpi, M., Moore, B., Quinn, T., Wadsley , J., Stadel, J., & Lake, G. 2001, ApJ, 559, 754

Moore, G., Lake, G., & Katz, N. 1998, ApJ, 495, 139

Mori, M., & Burkert, A. 2000, ApJ, 538, 559

Oemler, A., Dressler, A., & Butcher, H.R. 1997, ApJ, 474, 561

Pierce, M.J., & Tully, R.B. 1992, ApJ, 387, 47

Quilis, V., Moore, B., & Bower, R. 2000, Science, 288, 1617

Roberts, M.S., & Haynes, M.P. 1994, ARA&A, 32, 115

Ryden, B., Terndrup, D.M., Pogge, R.W., & Lauer, T.R. 1999, ApJ, 517, 650

Sadler, E.M., Oosterloo, T.A., Morganti, R., & Karakas, A. 2000, AJ, 119, 1180

Sandage, A., & Hoffman, G.L. 1991, ApJ, 379, 45L

Sandage, A., Binggeli, B., & Tammann, G.A. 1985, AJ, 90, 1759

Sandage, A., & Brucato, R. 1979, AJ, 84, 472

Sandage, A. 1986, A&A, 161, 89

Sage, L.J., Welch, G.A., & Mitchell, G.F. 1998, ApJ, 507, 726

Solanes, J. M. Marique, A., García-Gómez, C., González-Casado, G., Giovanelli, R., & Haynes, M. 2001, ApJ, 548, 97

Spitzer, L. 1958, ApJ, 127, 17

Tormen, G. 1997, MNRAS, 290, 411

Trentham, N. Tully, R.B., & Verheijen, M.A.W. 2001, MNRAS, 325, 385

Tully, R.B., & Fisher, J.R. 1977, A&A, 54, 661

Tully, R.B., & Fouqué, P. 1985, ApJS, 58, 67

Tully, R.B., & Shaya, E.J. 1984, ApJ, 281, 31

van Driel, W., & van Woerden, H. 1989, A&A, 225, 317

van Driel, W., Ragaigne, D., Boselli, A., Donas, J., & Gavazzi, G. 2000, AJ, 144, 463

van Zee, L., Haynes, M.P., Giovanelli, R. 1995, AJ, 109, 990

van Zee, L., Skillman, E.D., & Salzer, J.J. 1998, AJ, 116, 1186

Vigroux, L., Lachieze-Rey, M., Thuan, T.X., & Vader, J.P. 1986, AJ, 91, 70

Volders, L.M.J.S., & Högborn, J.A. 1961, BAN, 15, 307

Vollmer, B., Cayatte, V., Balkowski, C., & Duschl, W.J. 2001, ApJ, 561, 708

Wechsler, R.H., Bullock, J., Primack, J.R., Kravtsov, A.V., & Dekel, A. 2002, ApJ, 568, 52

White, S.D.M., & Frenck, C.S. 1991, ApJ, 379, 52

Worthey, G. 1994, ApJS, 95, 107

Young, L.M., & Lo, K.Y. 1997, ApJ, 476, 127

Young, L.M. 1999, AJ, 117, 1758

TABLE 1
Arecibo Sample

Name	R.A. (J2000)	Dec. (J2000)	Morphology[a]	m(B)[a]	Velocity[b] km s^{-1}	Integration Time ks	3σ Limit[c] mJy channel^{-1}
VCC 9	12:09:22.3	+13:59:33	dE1,N	13.9	1804±49	2.40	0.020
VCC 200	12:16:33.9	+13:01:56	dE2,N	14.7	65±43	1.80	0.044
VCC 303	12:18:42.8	+05:47:27	dE2?,N	15.8	2846±43	2.40	0.006
VCC 390	12:20:04.4	+05:24:57	dE3	16.9	2479±38	1.20	0.062
VCC 437	12:20:48.1	+17:29:16	dE5,N	14.5	1474±46	2.70	0.018
VCC 490	12:21:38.8	+15:44:42	dS0,N	14.3	1293±29	0.60	0.056
VCC 543	12:22:19.5	+14:45:39	dE5	14.8	861±58	5.70	0.002
VCC 546	12:22:21.6	+10:36:07	dE6	15.7	2067±104	2.40	0.004
VCC 817	12:25:37.7	+15:50:06	dE1	15.0	1086±57	3.00	0.016
VCC 856	12:25:57.9	+10:03:14	dE1,N	14.4	972±32	3.30	0.018
VCC 951	12:26:54.4	+11:40:06	dE2p,N	14.2	2066±21	1.80	0.020
VCC 953	12:26:54.6	+13:33:57	dE5?p,N	15.7	-629±65	2.40	0.010
VCC 1261	12:30:10.4	+10:46:46	dE5,N	13.7	1850±30	2.40	0.140
VCC 1351	12:31:17.5	+13:49:42	dE4	16.0	187±48	1.20	0.052
VCC 1713	12:37:29.0	+04:45:02	dE	15.1	1655±25	1.50	0.068
VCC 1743	12:38:06.6	+10:05:01	dE6	15.1	1279±51	2.40	0.008
VCC 1870	12:41:15.3	+11:17:55	dE6	15.8	1617±27	2.04	0.010
VCC 1890	12:41:46.3	+11:29:15	dE4p	14.8	1227±57	2.04	0.026
VCC 1919	12:42:19.0	+10:34:04	dE0,N	17.0	1869±54	1.80	0.070
VCC 1948	12:42:58.0	+10:40:55	dE3	15.1	1581±22	2.40	0.024
VCC 1971	12:43:31.0	+11:02:50	dE3:	16.6	1376±34	1.20	0.052
VCC 2019	12:45:20.4	+13:41:33	dE4,N	14.6	1895±44	2.70	0.022

[a]From Binggeli et al. (1995).
[b]From Conselice et al. (2001).
[c]The 3σ detection limit at the 1.3 km s^{-1}resolution.

TABLE 2

Dwarf Elliptical-like Low-Mass Cluster Galaxies in Virgo with HI Observations

Name	Alt. ID	R.A.(J2000.0)	Dec. (J2000.0)	Type[a]	B_m	v(km/s)	HI Detection	Source[b]
VCC 9	IC 3019	12:09:22.3	+13:59:33	dE1,N	13.93	1804±49	N	1
VCC 31		12:10:56.7	+09:13:07	dE	14.87	2215±40	Y	2,3
VCC 168		12:15:54.3	+14:01:26	dE2	17.0	682±10	Y	4
VCC 200		12:16:33.9	+13:01:56	dE2,N	14.69	65±43	N	1
VCC 216	IC 3097	12:17:01.2	+09:24:32	dE5,p,N	14.9	1325±79	N	6,7
VCC 303		12:18:42.8	+05:47:27	dE2?,N	15.8	2846±43	N	1
VCC 390		12:20:04.4	+05:24:57	dE3	16.9	2479±38	Y	1
VCC 405		12:20:18.1	+05:59:57	dE0	20.0	2097	Y	8
VCC 437	UGC 7399A	12:20:48.1	+17:29:16	dE5,N	14.54	1474±46	N	1
VCC 490		12:21:38.8	+15:44:42	dS0,N	14.3	1293±29	N	1
VCC 543	UGC 7436	12:22:19.5	+14:45:39	dE5	14.77	861±58	N	1
VCC 546		12:22:21.6	+10:36:07	dE6	15.7	2067±104	N	1
VCC 608	NGC 4322	12:23:01.7	+15:54:21	dE4,N	14.70	1803±100	Y	7
VCC 786	IC 3305	12:25:14.5	+11:50:57	dE7,N	15.11	2388±30	N	9
VCC 797		12:25:24.2	+18:08:29	dE3,N	17.0	773±8	Y	10
VCC 817	IC 3313	12:25:37.7	+15:50:06	dE1	15.0	1086±57	N	1
VCC 856	IC 3328	12:25:57.9	+10:03:14	dE1,N	14.42	972±32	N	1
VCC 917	IC 3344	12:26:32.4	+13:34:43	dE6	14.8	1375±66	N	7
VCC 940	IC 3349	12:26:47.1	+12:27:15	dE1,N	14.78	1563±57	N	9
VCC 951	IC 3358	12:26:54.4	+11:40:06	dE2p,N	14.23	2066±21	N	1
VCC 953		12:26:54.6	+13:33:57	dE5?p,N	15.70	-629±65	N	1
VCC 965	IC 3363	12:27:02.9	+12:33:37	dE7,N	15.40	790±50	N	9
VCC 990	IC 3369	12:27:17.1	+16:01:30	dE4,N	14.81	1727±34	N	7
VCC 1036	NGC 4436	12:27:41.6	+12:18:59	dE6,N	14.03	1163±50	N	7
VCC 1104	IC 3388	12:28:27.9	+12:49:24	dE5,N	15.31	1704±31	N	7
VCC 1122	IC 3393	12:28:41.7	+12:54:57	dE7,N	14.82	436±29	N	7
VCC 1261	NGC 4482	12:30:10.4	+10:46:46	dE5,N	13.66	1850±30	N	1
VCC 1348	IC 3443	12:31:15.7	+12:19:54	dE0p,N	15.64	1679±39	N	2
VCC 1351		12:31:17.5	+13:49:42	dE4	16.0	187±48	N	1
VCC 1355	*IC 3442	12:31:20.0	+14:06:53	dE2,N	14.31	1332±63	N	11
VCC 1386	IC 3457	12:31:51.3	+12:39:21	dE3,N	14.43	1426±60	N	7, 12
VCC 1491	*IC 3486	12:33:14.0	+12:51:28	dE2,N	14.8	903±42	N	7
VCC 1567	IC 3518	12:34:30.9	+09:37:28	dE5,N	14.64	1440±55	N	7,12
VCC 1713		12:37:29.0	+04:45:02	dE	15.1	1655±25	Y	1
VCC 1743	IC 3602	12:38:06.6	+10:05:01	dE6	15.1	1279±51	N	1
VCC 1826	IC 3633	12:40:11.2	+09:53:46	dE2,N	14.87	2033±30	N	7
VCC 1857	IC 3647	12:40:53.2	+10:28:33	dE4,N?	14.33	634±69	N	7, 12
VCC 1870		12:41:15.3	+11:17:55	dE6	15.8	1617±27	N	1
VCC 1876	IC 3658	12:41:20.4	+14:42:02	dE5,N	14.85	45±49	N	7
VCC 1890	IC 3665	12:41:46.3	+11:29:15	dE4p	14.84	1227±57	N	1
VCC 1910	IC 809	12:42:07.8	+11:45:16	dE1,N	14.17	206±26	N	7
VCC 1919		12:42:19.0	+10:34:04	dE0,N	17.0	1869±54	N	1
VCC 1948		12:42:58.0	+10:40:55	dE3	15.1	1581±22	N	1
VCC 1949	NGC 4640	12:42:58.1	+12:17:10	dE6,N	14.19	2077±75	Y	5,7,9
VCC 1971		12:43:31.0	+11:02:50	dE3:	16.6	1376±34	N	1
VCC 2019	IC 3735	12:45:20.4	+13:41:33	dE4,N	14.55	1895±44	N	1
VCC 2050	IC 3779	12:47:20.7	+12:09:59	dE5,N	15.2	1367±75	N	7
VCC 2062		12:47:59.9	+10:58:33	dE	19.0	1146±8	Y	13, 14

[a] Morphological types are from the estimates given by Binggeli, Sandage & Tammann (1985)

[b] (1) This paper, (2) van Driel et al. (2000), (3) van Zee et al. (1995), (4) Hoffman et al. (1987), (5) Bottinelli et al. (1990), (6) Bothun et al. (1985), (7) Huchtmeier et al. (1986), (8) Duprie & Schneider (1996), (9) Haynes & Giovannelli (1986), (10) Burstein et al. (1987), (11) Lake & Schommer (1984), (12) Schneider et al. (1990), (13) Cayatte et al. (1990), (14) Hoffman et al. (1993)

TABLE 3
PROPERTIES OF HI DETECTED LMCGs

Name	M_B	W_{50} (km s^{-1})	W_{20} (km s^{-1})	$\int Sdv$ (Jy × km s^{-1})	M_{HI} 10^9 $M_\odot$	M_{HI}/L_B $M_\odot$ /$L_{\odot,B}$	R[a] (kpc)	M_{dyn} $M_\odot \times 10^9$	f_{gas}[b]	M_{dyn}/L_B $M_\odot$ /$L_{\odot,B}$
VCC 31	-16.4	142	132	1.53	0.12	0.21	1.2	1.4	0.08	2.4
VCC 168	-14.3	50	64	0.34	0.03	0.33	1.4	0.2	0.12	2.5
VCC 390	-14.4	285±7	286±5	0.8±0.01	0.06	0.68	0.8	4	0.02	45
VCC 405[c]	-11.5	282	···	1.1	0.08	8.4	0.5	2.2	0.04	218
VCC 608	-16.6	88	195	16	1.22	1.8	3.8	1.7	0.72	2.5
VCC 797	-14.3	28	···	0.40	0.03	0.38	1.2	0.1	0.57	0.6
VCC 1713	-16.2	46±8	60±6	1.1±0.004	0.08	0.20	1.4	0.2	0.56	0.4
VCC 1949	-17.1	233	304	5.5	0.42	0.38	6.3	79.0	0.02	18
VCC 2062[d]	-12.3	87	···	7.2	0.55	55	1.8	0.8	0.72	78

[a]Radii measurements are from Binggeli et al. (1985).
[b]Fraction of gas in HI, defined as M_{HI}/M_{dyn}.
[c]Likely a spurious HI detection (see §3.5.3).
[d]This object is probably a pure dwarf irregular (§3.5.7).

TABLE 4
QUANTITATIVE MORPHOLOGICAL PROPERTIES OF HI DETECTED LMCGS

Name[a]	A[b]	C[c]	S[d]	n[e]	$r_0('')$[e]	r_0 (kpc)
VCC 31	-0.02±0.10	2.44	0.02±0.13	1.27±0.01	4.4±0.03	0.38±0.00
VCC 168	0.00±0.17	2.63	-0.04±0.09	1.28±0.02	7.4±0.09	0.64±0.01
VCC 390	-0.08±0.11	2.95	-0.14±0.11	0.95±0.01	3.3±0.04	0.29±0.00
VCC 797	-0.02±0.05	2.69	0.16±0.06	0.80±0.01	2.8±0.07	0.24±0.01
VCC 1713	-0.04±0.08	2.54	0.07±0.05	1.20±0.03	29.8±0.33	2.6±0.03

[a]Object name from the Virgo Cluster Catalog (Binggeli et al. 1985)

[b]Asymmetry index, A, as defined and measured by Conselice et al. (2000a). See Conselice et al. (2000b) and Conselice (2003) for further interpretations of this index

[c]Concentration index, C, as defined in Bershady et al. (2000). Higher values of this index ($\sim$ 4) are typically found for giant ellipticals while disk and dwarf galaxies have values ($\sim$ 2 - 3)

[d]Clumpiness index, S, as defined in Conselice (2003).

[e]The Sérsic index, n and scale length r_0 as defined in §3.2. Scale lengths are converted from arcseconds into kpc assuming a distance of 18 Mpc to the Virgo cluster

TABLE 5

Averages Properties and Dispersions for Different Populations

	$<M_B>$	$<M(HI)>$ $M_\odot \times 10^9$	$<f_{gas}>$[a]	$<M_{HI}/L_B>$ $M_\odot/L_{\odot,B}$
HI LMCGs [b]	-15.4±1.2	0.28±0.44	0.30±0.28	0.57±0.57
Virgo Irr[c]	-16.4±0.8	0.52±0.98	···	0.61±0.54
Virgo Amorphous[c]	-17.4±1.0	0.12±0.13	···	0.07±0.05
LG Irr[d]	-14.5±2.7	0.20±0.26	0.30±0.24	1.4±1.7
LG dE[d]	-13.7±2.2	$3\pm6\times10^{-4}$	$1.5\pm4\times10^{-3}$	0.001±0.002
LG TT[e]	-10.8±1.0	$2\pm2\times10^{-3}$	0.15±0.21	0.44±0.28
LG Spiral[d]	-19.3±0.9	4.2±2.3	0.11±0.11	0.54±0.38

[a]Defined as in Table 3, as the fraction of the total mass contained in HI gas, where the total mass is approximated by M_{dyn}.

[b]From the data presented in this paper, especially Table 3.

[c]Based on the observational data presented in Gallagher & Hunter (1989).

[d]From data in van den Bergh (2000) and Mateo (1998).

[e]Transition types (TT) include the following galaxies: Antila, Aquarium (DDO 210), LGS-3 (Pisces), Phoenix, Pegasus, DDO 155, DDO 216. The data are from van den Bergh (2000) and Mateo (1998).

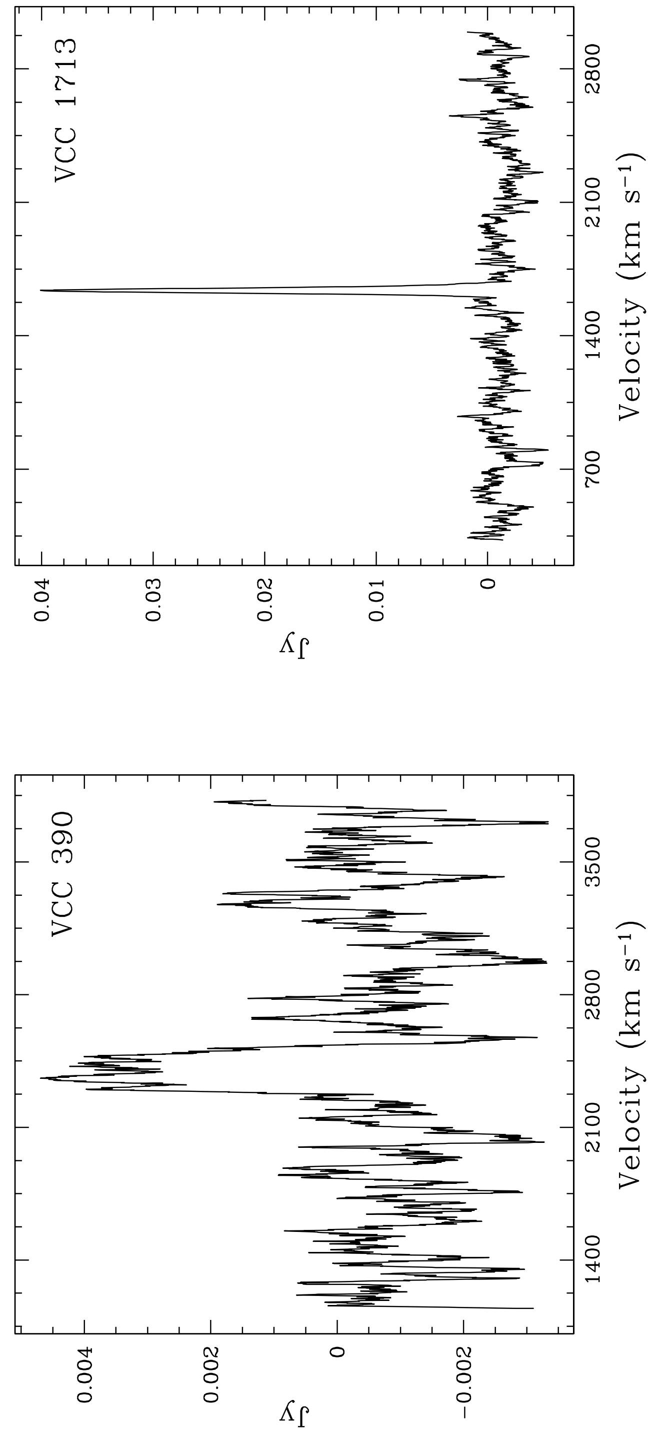

Fig. 1.— Arecibo HI spectra of our two objects with HI detections, VCC 390 and VCC 1713.

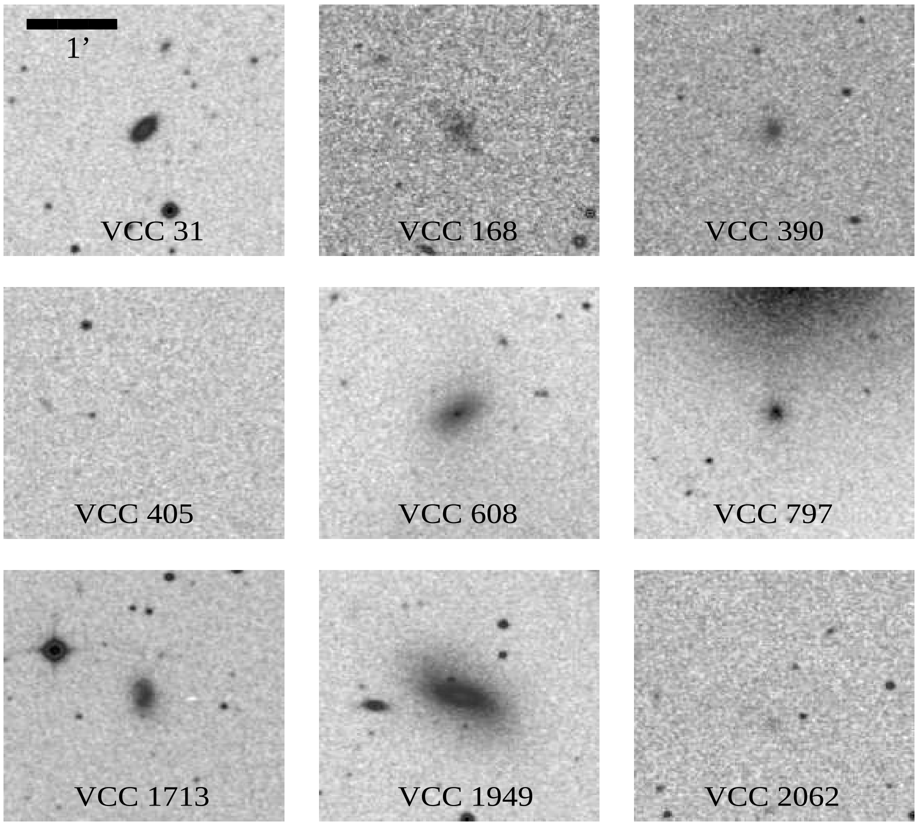

Fig. 2.— Palomar sky survey images centered on the nine candidate dEs with HI detections. The size of these images matches the beam of the Arecibo telescope at the 21 cm wavelength ($\sim 3'$).

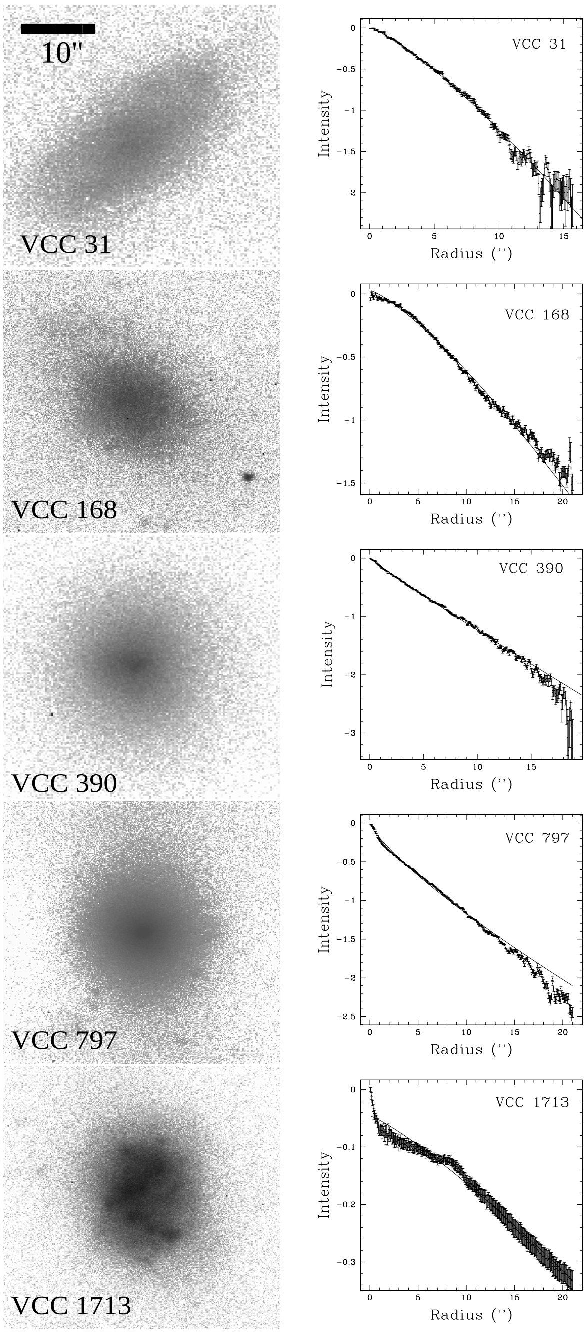

Fig. 3.— Images and surface brightness profiles for the five objects detected in HI, imaged with the WIYN 3.5 meter telescope in the R-band. The intensity is log-normalized to zero at the peak intensity and all images are $\sim 35''$ on a side, with the scale indicated by the bar on the top panel.

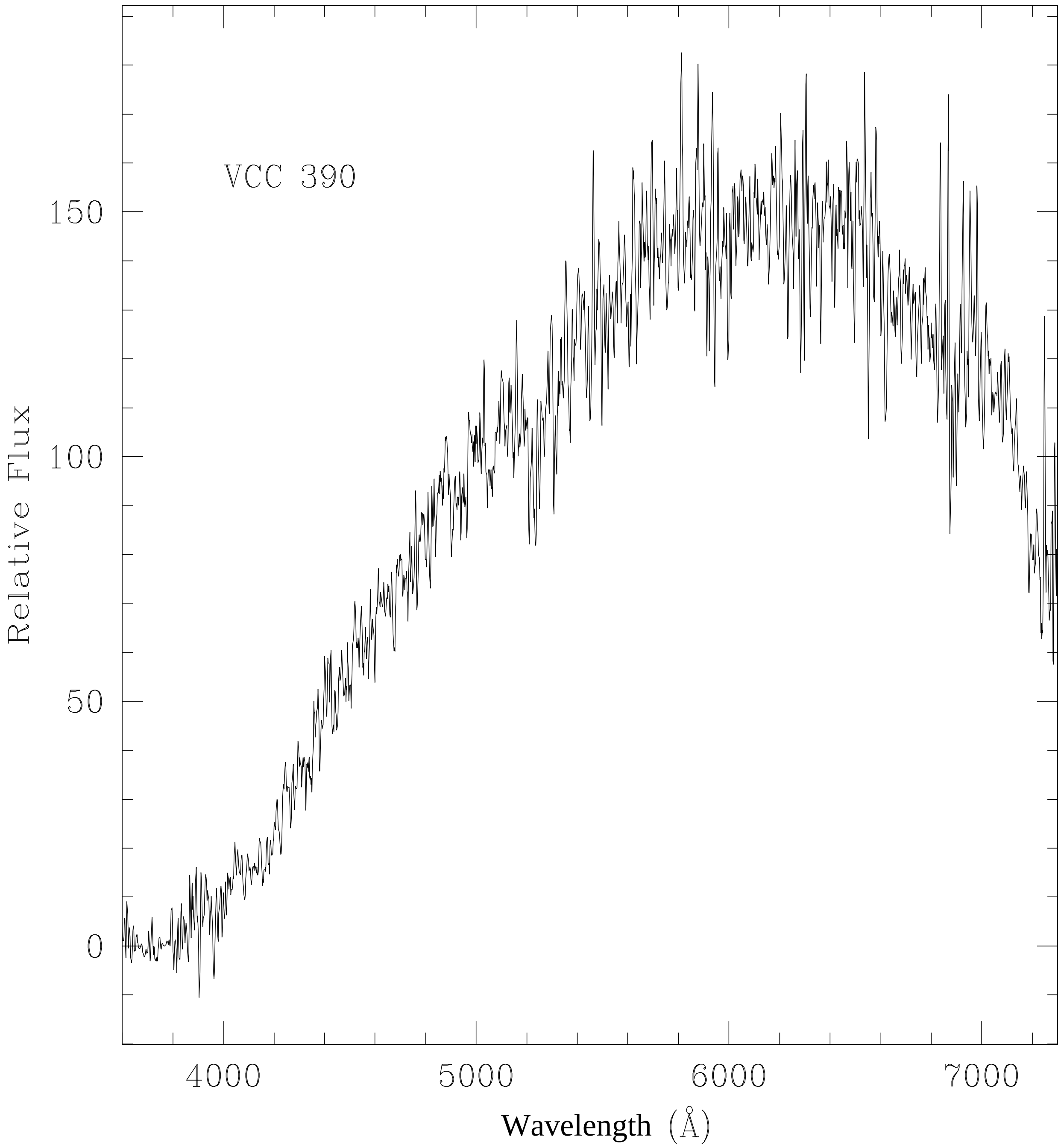

Fig. 4.— Optical spectrum of the dwarf elliptical galaxy VCC 390, taken with the WIYN 3.5m telescope with an arbitrary flux normalization.

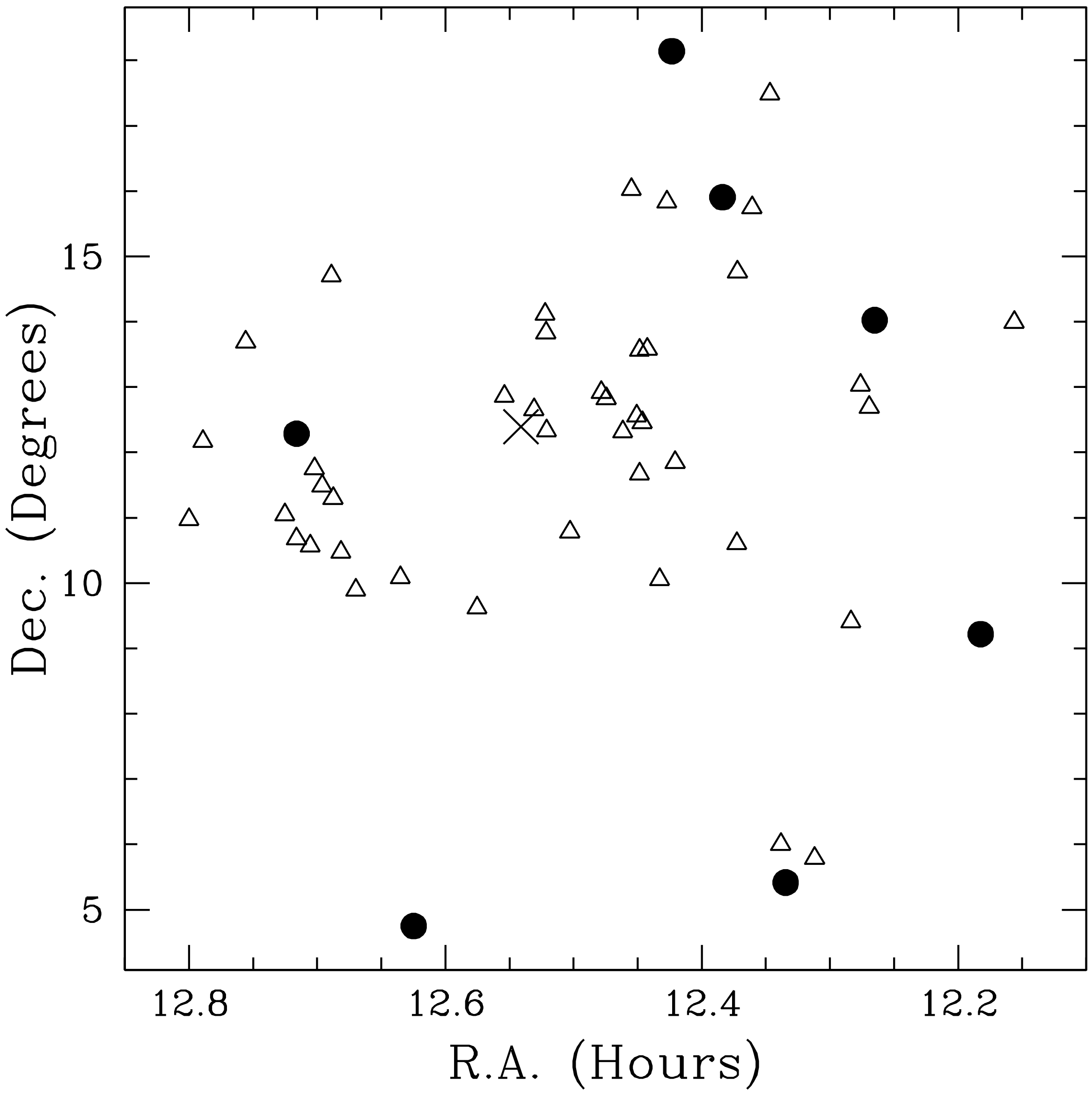

Fig. 5.— The distribution on the sky of dEs observed at 21-cm in the Virgo cluster. The open triangles represent non-detections while the solid circles are the location of the dEs with detected HI. The cross toward the center is the location of the giant elliptical M87.

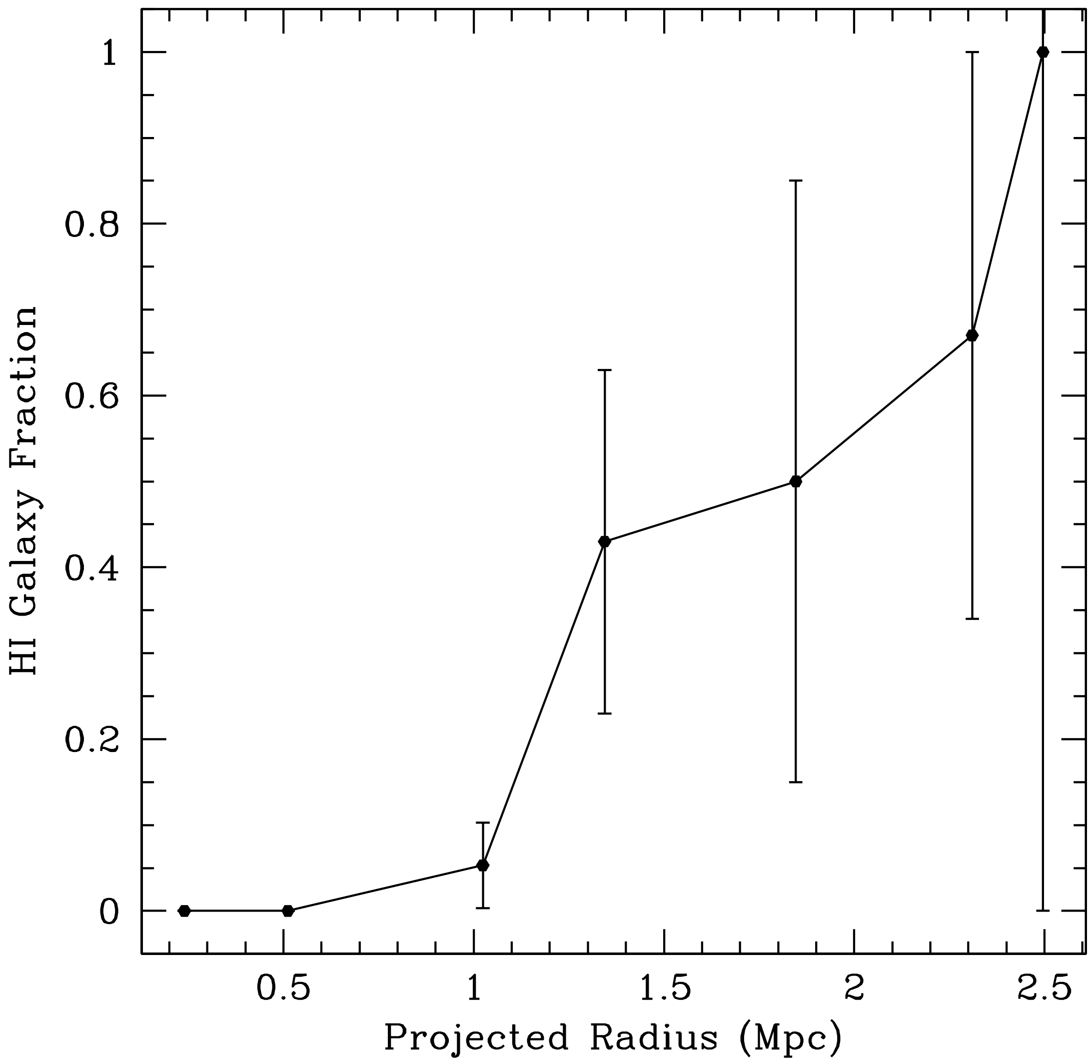

Fig. 6.— The fraction of Virgo classified dwarf elliptical galaxies detected in HI as a function of projected distance from the center of the cluster.

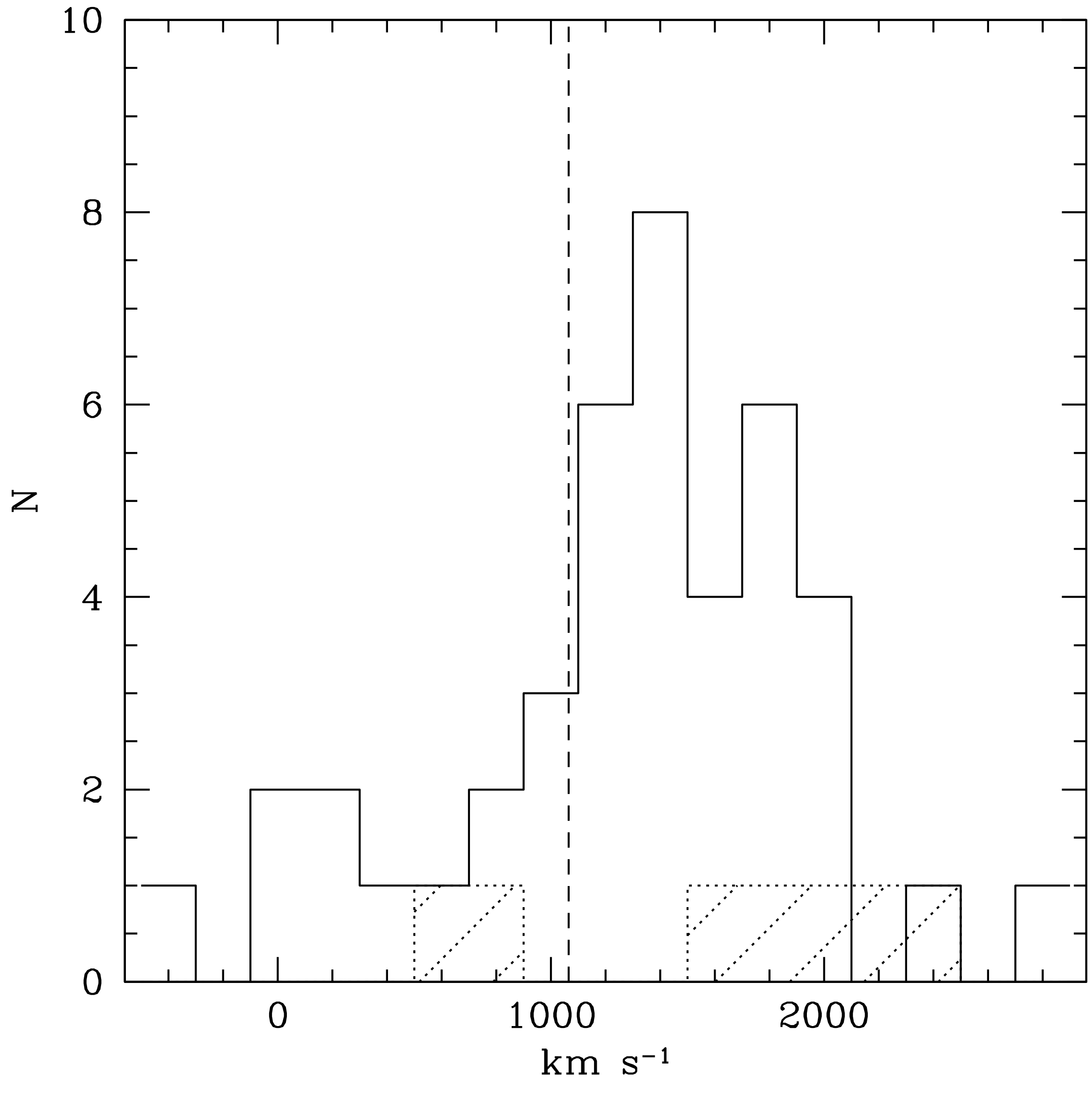

Fig. 7.— Histogram of radial velocities for dEs searched for in HI. The open histograms represent the dE non-detections, while the shaded histogram is for Virgo dEs with HI detections. The vertical dashed line shows the mean velocity of the Virgo cluster, from Paper I.

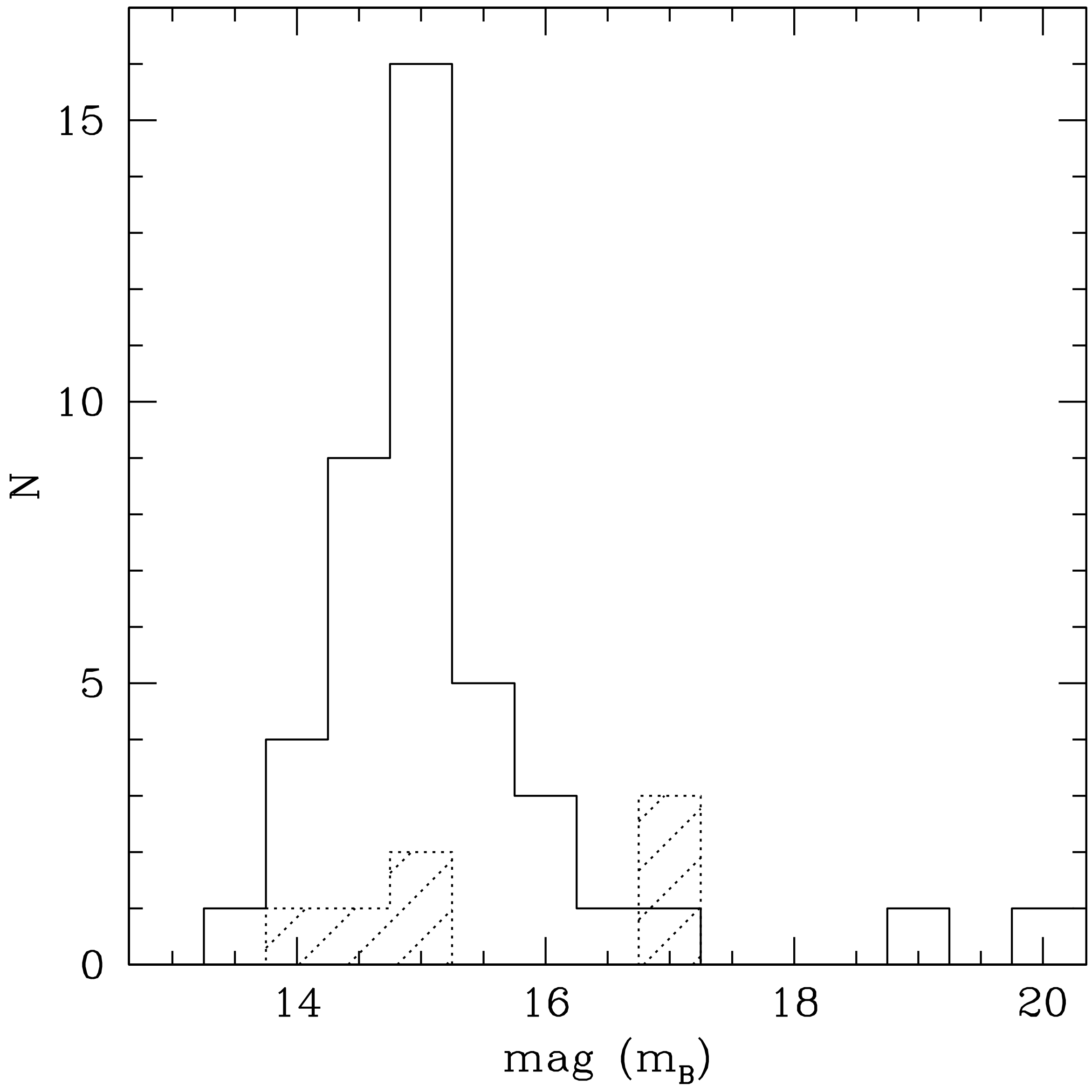

Fig. 8.— Histograms of apparent B-band magnitudes for non-detected (open) and HI detected (shaded) Virgo cluster dEs. The shadings are the same as in Figure 7.

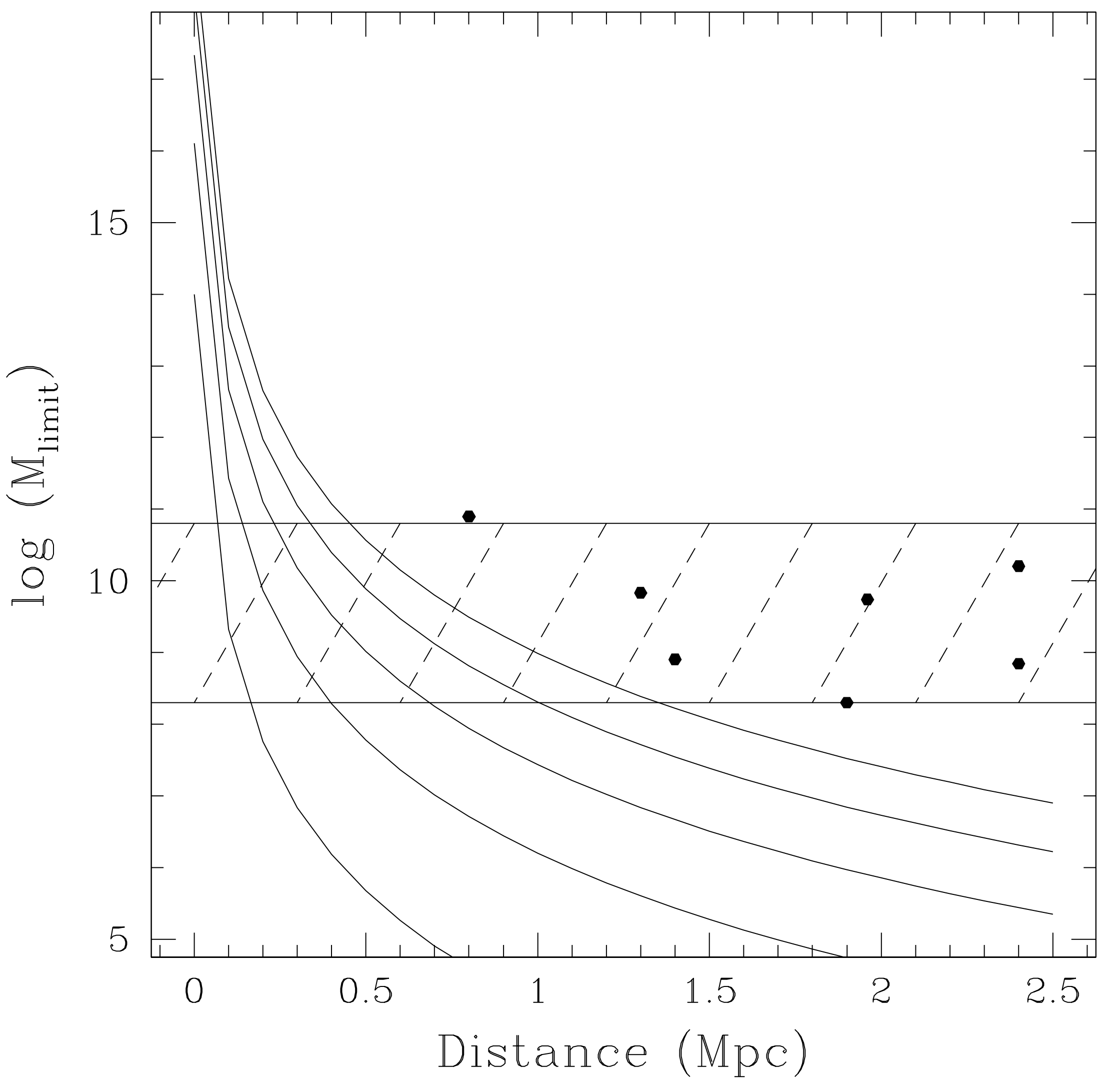

Fig. 9.— Relationship between the minimum galaxy mass, $M_{\rm limit}$, above which HI gas is expected to survive ram-pressure stripping, as a function of distance from the Virgo cluster center. The five solid lines show this relationship for galaxy orbital velocities relative to the ICM of v = 250, 500, 750, 1000 and 1250 km s^{-1} at increasing mass limits. The solid points show the projected locations of the seven HI LMCGs studied in this paper which are all above the minimum mass limits. The hatched region shows the range of total masses for our HI LMCGs, and dwarf galaxies in general.

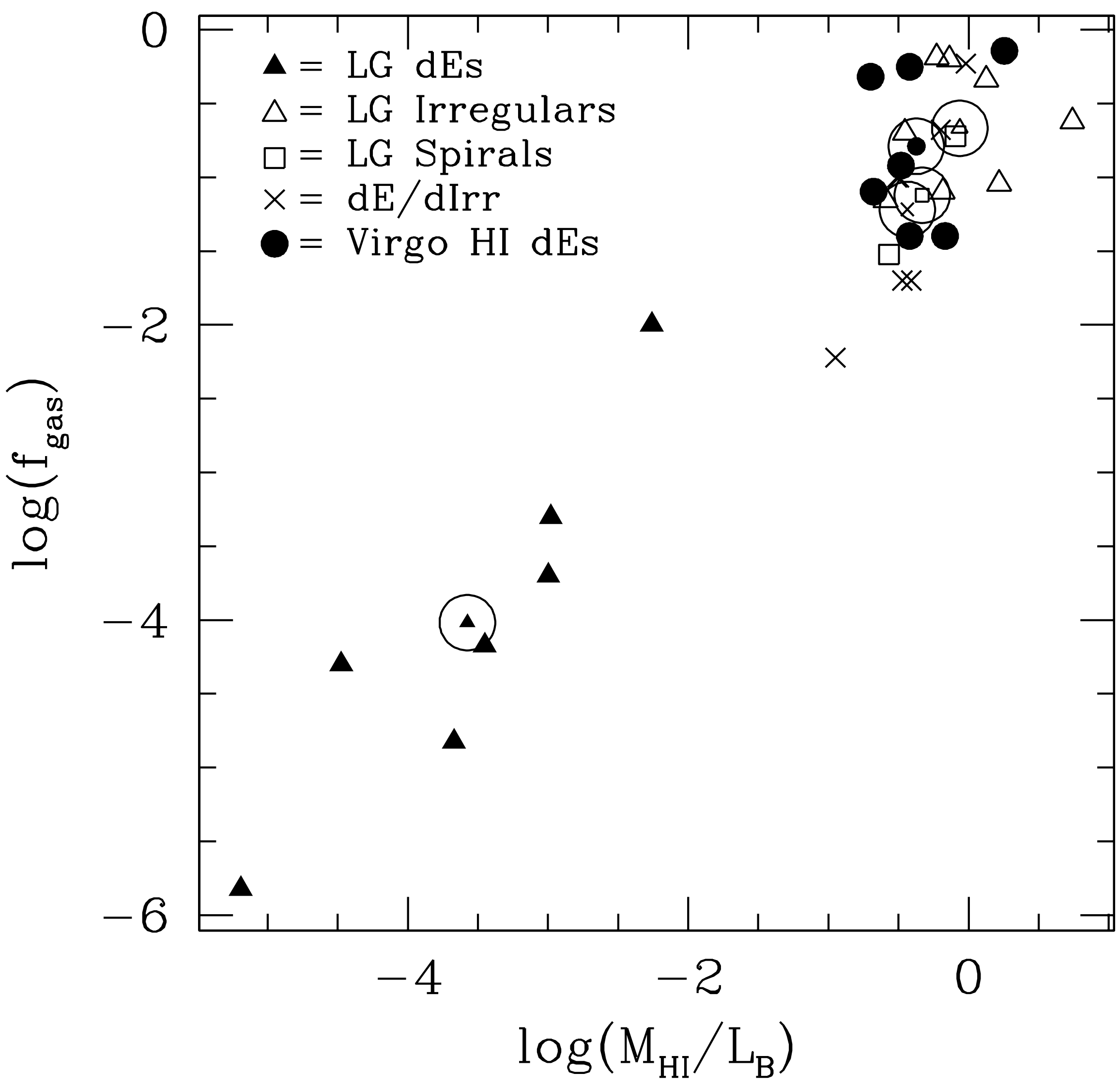

Fig. 10.— The fraction of mass in HI (f_{gas}) for various Virgo cluster member galaxy types plotted as function of M_{HI}/L_B. Each separate galaxy population is designated by the labeled symbols. The average position for each type is plotted as a small version of its respective symbol in a circle.

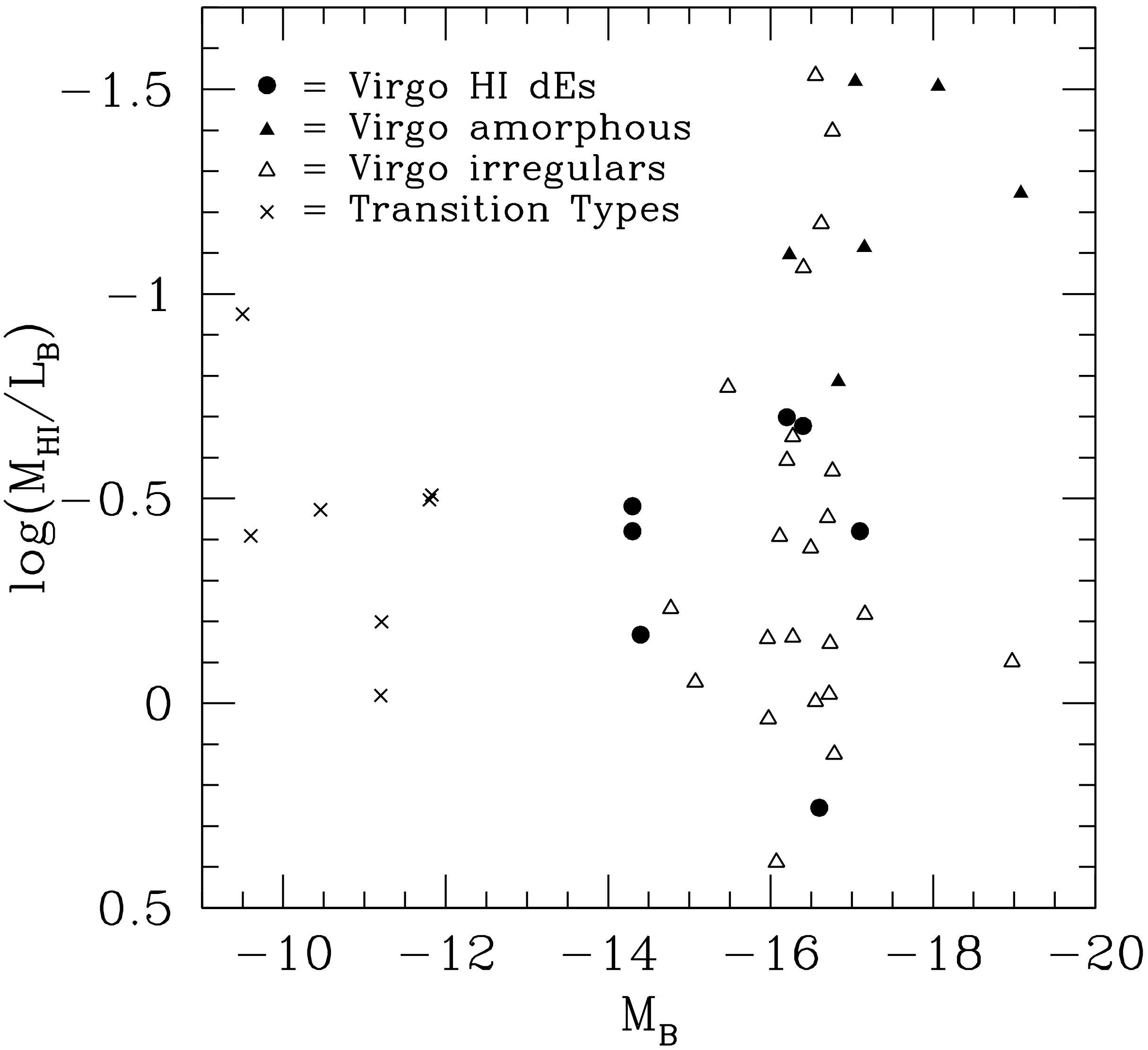

Fig. 11.— The absolute magnitude (M_B) vs. M_{HI}/L_B diagram for various galaxy populations, including Virgo irregular and amorphous galaxies from Gallagher & Hunter (1989), the dE HI sample studied in this paper, and dwarf transition types in the Local Group.

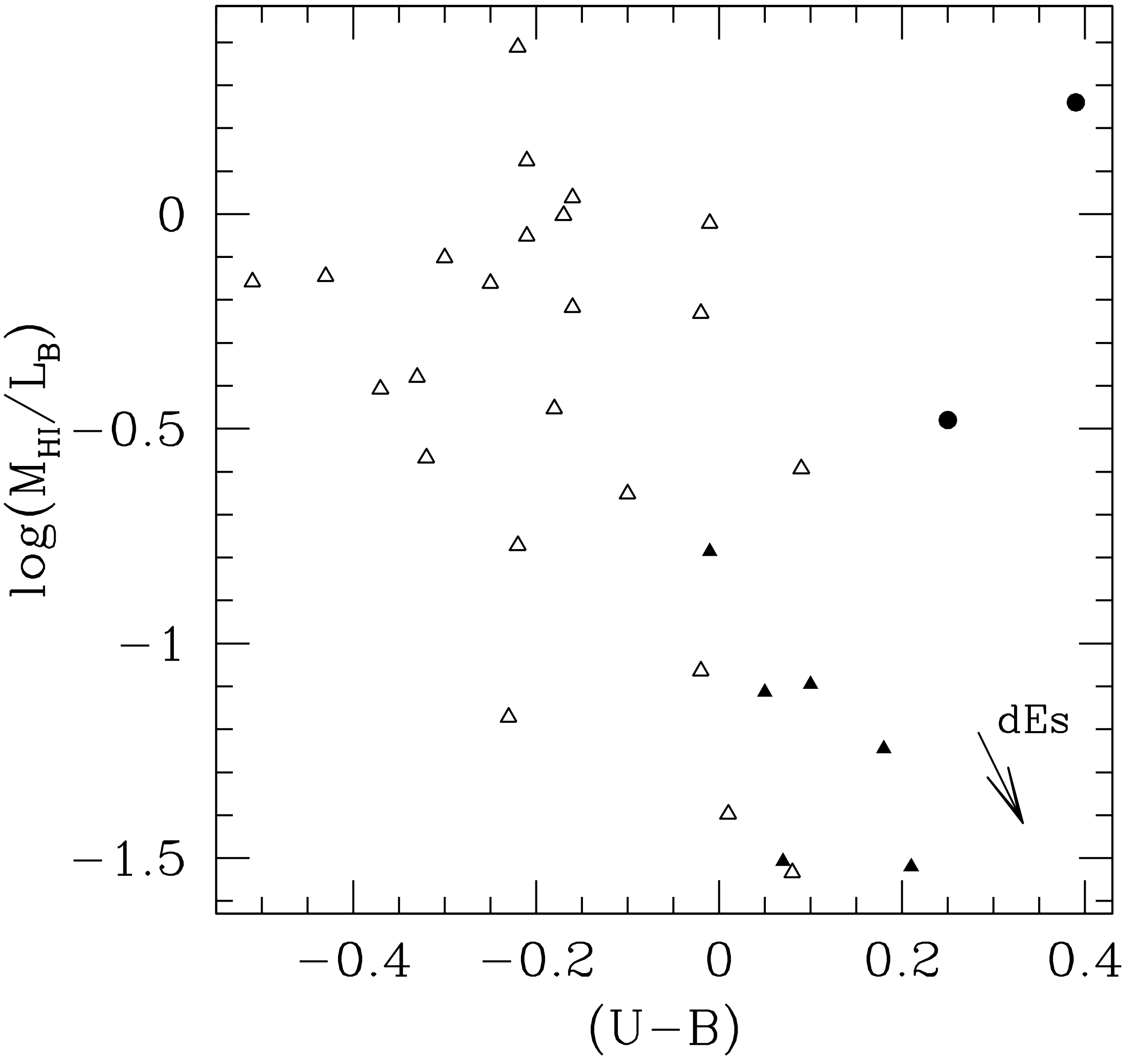

Fig. 12.— Diagram of M_{HI}/L_B vs. $(U-B)$ color for the irregular (open triangle) and amorphous (solid triangle) Virgo galaxy sample from Gallagher & Hunter (1986). The two HI detected LMCGs with both M_{HI}/L_B and derived $(U-B)$ colors, VCC 168 and VCC 608, are plotted as solid circles.

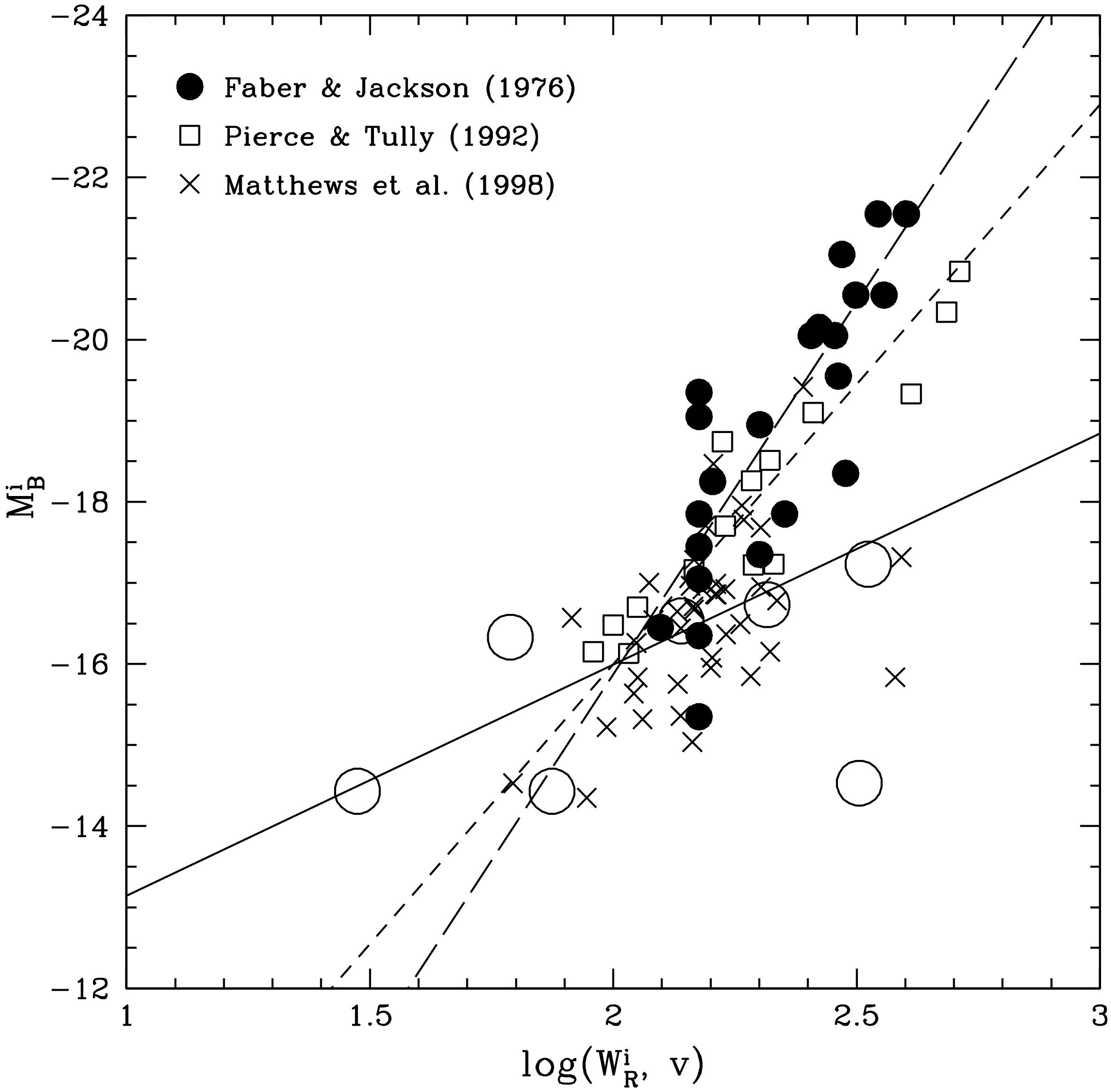

Fig. 13.— The velocity line-width (W_R^i) or velocity dispersion (v) vs. luminosity (M_B^i) relationship for various types of galaxies. The solid circles are the galaxies from the sample in Faber & Jackson (1976) and the open boxes are from the sample used in Pierce & Tully (1992). The long dashed line is a fit to the Faber-Jackson points, while the short dashed line is the Tully-Fisher relationship and the crosses are for the extreme late-type disk galaxies from Matthews et al. (1998). The open circles are the LMCGs after correcting their velocities for inclination and removing in quadrature a minimum value for turbulence, $W_t = 5$ km s^{-1}.